Energy Conversion and Management 153 (2017) 391–408

Contents lists available at ScienceDirect

Energy Conversion and Management

journal homepage: www.elsevier.com/locate/enconman

Optimisation of stand-alone hybrid CHP systems meeting electric and heating loads

Barun K. Das*, Yasir M. Al-Abdeli

School of Engineering, Edith Cowan University, Joondalup, WA 6027, Australia

ARTICLE INFO

Keywords:
PV
ICE
MGT
Electric load
Heating load
CHP

ABSTRACT

Most research published into stand-alone energy systems, hybridised by supplementing PV with combustion-based prime movers, considers meeting an electric load demand. This paper goes further by studying the role of both electric and heating loads on the optimisation of hybridised stand-alone Combined Heating and Power (CHP) systems. The role of both the load following strategy in these systems (electric only FEL, versus electric and thermal FEL/FTL) as well as the relative magnitude of the heating load is analysed on system cost and performance. The conceptual CHP systems modelled also consider waste system derived from either multiple Internal Combustion Engines (ICEs) or Micro Gas Turbines (MGTs). The research uses MATLAB-based Genetic Algorithm (GA) optimisation throughout and features detailed hardware characteristics as well as temporally fluctuating meteorological (solar irradiance, temperature) and load (electric, heating) data. The outcomes are also tested in relation to CHP systems sized whilst optimising either single (Cost of Energy-COE, $/kW h) or multiple functions (COE and overall system efficiency, η_{CHP},%).

Results indicate that whilst the power management strategy used in CHP systems (FEL or FEL/FTL) has minimal effects on the COE, it can appreciably affect other performance indicators. For example, in CHP systems sized based on FEL/FTL, whilst COE = ~0.20 $/kW h the resulting η_{CHP} is 66% for PV/Bat/ICE and 44% for PV/Bat/MGT. This is compared to using a PMS of the FEL type which results in similar COE = ~0.21 $/kW h but with η_{CHP} = 50% in PV/Bat/ICE systems and 34% in PV/Bat/MGT. In relation to overall environmental impact expressed though Life Cycle Emission-LCE (kg CO_2-eq/yr) when heating demand is around 50% of the electric (Electric to Thermal Load Ratio = 60:40), a PMS of the FEL/FTL results in up to 30% lower LCE compared to those with FEL in some CHP systems.

1. Introduction

Energy usage is a key indicator of national development with the major sources being conventional fossil fuels such as coal, petroleum oil, and natural gas. However, limited reserves of fossil fuels and the environmental emissions from burning them have forced policy makers to deploy more alternative energy sources. Unlike conventional sources, renewables produce negligible operational GHG emissions and can theoretically be generated worldwide. Even though the application of renewable energy in electricity generation has increased significantly [1–3], due to its seasonal and temporal variations neither PV nor wind can reliably satisfy the load demand [4,5]. Therefore, many stand-alone systems integrate combustion based prime movers such as Internal Combustion Engines (ICEs) or Micro Gas Turbines (MGTs) alongside renewables. These hybridised energy systems also include energy storage media (batteries, hydrogen, capacitors) since renewable energy resources are inherently intermittent [6–13]. Thus, much reliance remains on conventional fossil fuel based power generation units. However, in relation to stand-alone hybrid systems, very few research studies are available in literature which examine their optimisation when waste heat recovery exists in the context of cogeneration or trigeneration [14–18].

A combustion powered stand-alone (completely off-grid) or distributed (occasional access to grid) cogeneration system, commonly known as Combined Heat and Power (CHP), involves the simultaneous production of heat and power from a single fuel source to meet an electric and heating load. In contrast, trigeneration additionally meets a cooling load along with the CHP application for a similar fuel usage. These systems which are commonly termed Combined Cooling, Heating, and Power (CCHP) provide improved power quality and reliability, save energy, reduce net emissions [19–24]. However, the vast majority of these systems do not integrate renewables [25–28]. As such, a conventional power plant transforms around 35–55% of the fuel's energy into electric power and the rest is released to the environment as

* Corresponding author at: School of Engineering, Edith Cowan University, 270 Joondalup Drive, WA 6027, Australia.
E-mail address: bdas@our.ecu.edu.au (B.K. Das).

http://dx.doi.org/10.1016/j.enconman.2017.09.078
Received 14 July 2017; Received in revised form 27 September 2017; Accepted 30 September 2017

Nomenclature

B_{SOC}	battery state of charge (%)
$B_{SOC,\ max}$	maximum battery state of charge (%)
$B_{SOC,\ min}$	minimum battery state of charge (%)
C_A	annualised cost ($)
C_{A_cap}	annualised capital cost ($)
C_{A_fuel}	annualised fuel cost ($)
$C_{A\_O\&M}$	annualised operation and maintenance cost ($)
C_b	nominal battery capacity (kW h)
C_{fuel_sup}	fuel consumption rate for supplementary prime movers (kg/h)
C_{fuel_ICE}	fuel consumption rate for ICE (kg/h)
C_{fuel_MGT}	fuel consumption rate for MGT (kg/h)
E_L	energy load demand (kW h)
E_s	useful energy production from the system (kW h)
E_{elec}	electrical energy demand (kW h)
E_{ther}	thermal energy demand (kW h)
F	objective function (Genetic Algorithm)
F_{sup}	fuel energy (kW)
G	inequality constraints (Genetic Algorithm)
H	equality constraints (Genetic Algorithm)
I_L	light current (A)
$I_{L,ref}$	short circuit current at reference temperature (A)
I_{mp}	maximum power point current (A)
I_o	diode reverse saturation current (A)
I_{PV}	saturation current (A)
I_{sc}	short circuit current (A)
LPS_{elec}	loss of power supply, i.e. reliability of meeting electric load (kW h)
LPS_{ther}	loss of power supply, i.e. reliability of meeting thermal load (kW h)
N_{batt}	number of lead acid batteries
N_{PV}	number of PV modules
N_{sup}	number of supplementary prime movers (ICE or MGT)
P_{elec}	electric load demand (kW)
P_{ICE}	power generation by ICE (kW)
P_L	total load demand (kW)
P_{MGT}	power generation by MGT (kW)
P_{NET}	net power generation (kW)
P_{PV}	power generation by PV (kW)
P_{sup}	power generation by supplementary prime movers (kW)
$P_{sup,min}$	minimum starting threshold of supplementary prime movers (kW)
P_{ther}	thermal load demand (kW)
P_{heat}	thermal load met by recoverable heat (kW h)
Q_{th}	recoverable heating energy (kW h)
R_s	series resistance (Ω)
R_{sh}	shunt resistance (Ω)
S	solar irradiation (W/m^2)
S_{ref}	reference solar irradiation (W/m^2)
T_{ref}	reference temperature (°C)
V	PV module voltage (V)
V_{oc}	nominal open circuit voltage (V)
V_{mp}	maximum power point voltage (V)

Greek symbols

α	modified ideality factor
β	lifetime equivalent CO_2 emission (kg CO_2-eq/kW h)
κ_t	temperature coefficient of short circuit current (/°C)
η_b	battery efficiency (%)
η_{CHP}	overall CHP efficiency (%)
η_{inv}	inverter efficiency (%)
$\eta_{wh,sys}$	overall process heater efficiency (%)

Abbreviations

CCHP	combined cooling, heating, and power
CHP	combined heating and power
COE	cost of energy ($/kW h)
ETLR	electric to thermal load ratio
FEL	following electric load
FTL	following thermal load
GA	genetic algorithm
ICE	internal combustion engine
LCE	life cycle emissions
LHV	lower heating value
LPS	loss of power supply (kW h)
LPSP	loss of power supply probability
MGT	micro gas turbine
PV	photovoltaic
PMS	power management strategy
RP	renewable penetration (%)
TER	thermal to electric ratio

waste heat. By introducing CHP, efficiency can exceed 90% [29,30] with 20–30% lesser fuel consumption. Additionally, approximately 50% fuel savings can be achieved for CCHP applications [31]. CHP systems can be operated on a topping cycle (electric energy first and recovered waste heat can then be used for thermal applications), bottoming cycle (thermal load is satisfied first and electric energy is then generated from surplus thermal energy), and combined cycle (produce additional electricity using recovered waste heat to run a steam turbine) [32]. Several different types of prime movers can be used in stand-alone CHP applications including ICE's, MGT's, and high temperature Fuel Cells (FC's). Incorporating a waste heat recovery system with these prime movers to meet local heating and cooling loads, can help achieve higher overall efficiency [33], with fewer environmental pollutants [34,35]. Caresana et al. [36] studied a 100 kW MGT system and found electrical efficiencies up to 29% when operating in power only made in the 80–100 kW range, but these could increase to an overall efficiency of about 74% when operating in CHP with substantially lower pollutants. Onovwiona et al. [37] used parametric modelling in a techno-economic analysis of an ICE based residential cogeneration system. Their investigation with three different ICE capacities (2 kW, 3.5 kW, and 6 kW), simulated these systems in 15 min time steps and revealed that electrical efficiency of 23.3% can be raised to almost 80% overall efficiency using CHP technology. However, any deficit in meeting electric and thermal demand had to be satisfied by resorting to the utility grid and an auxiliary burner. As such, their system was not stand-alone as with the current study.

Identifying the optimum sizing of stand-alone hybrid systems is a major challenge as several parameters must be concurrently considered, such as the choice of renewables, hardware/device characteristics, variations in load profiles, and the modelling methods used as well as their constraints and parameters. Because of the complexity and non-linearity involved in optimal sizing, artificial intelligence has been applied instead of conventional analytical methods [38]. Specifically, Genetic Algorithms (GAs) [39–44], Particle Swarm Optimization (PSO) [45–48], Artificial Neural Networks (ANN) [49], and Fuzzy Logic [46,50], have been extensively used for CHP and CCHP system optimisation. The Power Management Strategy (PMS) is another important parameter that can affect the optimal sizing. The most commonly used PMS's are: Following Electric Load (FEL), and Following Thermal Load (FTL) [51]. In the former, prime movers are operated to satisfy all

electricity demand, with the waste heat meeting part or all of the thermal demand and the rest being met by an auxiliary boiler. In the later, the system is operated to meet all the thermal demand but the electrical power produced by the generating unit can satisfy part (or all) of the electrical load, deficits likely to be imported from the grid [52]. Integration of PV with CHP systems potentially reduces emissions and increase reliability [53–55]. In this context, Brandoni et al. [54] evaluated a residential hybrid (PV) micro-CHP system but used non-adaptive linear programming. However, unlike the present paper which considers a stand-alone system, their system was dependant on grid electricity for additional power requirement as well as using additional hardware such as a boiler and vapour compression chiller to meet additional heating and cooling not satisfied by the CHP. Their detailed PMS, a consideration which can strongly impact the outcomes of any system optimisation was not reported. Ebrahimi et al. [50] alternatively used a multi-criteria sizing function to optimise the size of prime movers for a another residential micro-CCHP system and investigated thermodynamical parameters (fuel energy saving ratio, exergetic efficiency), economic criteria (net present value, internal rate of return, and payback period), and environmental parameters (CO_2, CO and NO_x reduction). They did not consider a dynamic load profile. In another study, Abdollahi et al. [40] performed multi-objective Genetic Algorithm (GA) optimisation for a residential CCHP system with exergetic efficiency, total levelized cost rate, and environmental cost rate as objective functions. The study considered a Micro Gas Turbine, Heat Recovery Steam Generator (HRSG), and an absorption chiller to meet cooling, heating, and electrical power. Their system was not stand-alone as it had an additional electric boiler and auxiliary chiller, both powered by a grid connection, for meeting peak demands. Moreover, their study only used a (coarse) monthly averaged load profile which also affects the operational characteristics and system efficiencies. Ahmadi et al. [42] reported a multi-objective optimisation of exergy efficiency, total cost, and CO_2 emission when modelling a 50 MW gas turbine supplying electric power and thermal energy in a CHP system in a paper mill. From the above it is evident that optimisation of stand-alone hybrid CHP systems based on ICE or MGT has not been received attention in the recent literature.

The main objectives of this paper are to (i) analyse the effects of various parameters on the optimal sizing of stand-alone hybridised CHP energy system meeting reliability constraints (both electric and thermal loads); (ii) highlight the impact of FEL or FEL/FTL Power Management Strategies on system sizing and operation; and (iii) compare between systems sized using single– vs multi–objective GA optimisation (minimising cost and maximising efficiency). To achieve this, the present study extends work done on CHP energy systems through simultaneously considering four aspects. Firstly, the system studied does not include auxiliary boilers to meet heating demand but solely relies on renewables and multiple units of supplementary prime movers (either ICE or MGT) to satisfy both P_{elec} (t) (electric) and P_{ther} (t) (thermal) loads. Whilst energy systems meeting an electric load (only) have been optimised when achieving a target load reliability constraint such as LPSP [56–59], considering LPSP into CHP systems which also meet a thermal demand has not been widely reported in the literature [51,60–65]. Additionally, this paper differs to others [37,54,66,67] in that the CHP systems analysed are stand-alone and not connected to a grid. Secondly, this research presents the intricate details of the Power Management Strategy used, which is not always done in earlier works. Moreover, the PMS deployed herein features varying relative magnitudes of P_{elec} (t) and P_{ther} (t) even when operating under FEL/FTL and FEL. In this context, it should be noted that despite PMS architectures affecting the performance of stand-alone energy systems [68], other CHP system studies [69,70] have not presented their PMS architectures (algorithms) to the same level of detail done in the present work. Thirdly, in this paper the outcomes of Genetic Algorithm system optimisation are compared between using single- (COE, $/kW h) or dual-objective functions (COE, $/kW h; and η_{CHP},%), whilst other studies using GA to analyse CHP systems [23,42–44] neither contrast between single- and multi-objectives (for the same hardware) nor do they feature Cost of Energy (COE) and overall efficiency (η_{CHP}). Fourthly, the simulations undertaken are applied to systems which are highly dynamic as they are based on 15 min temporal resolution, compared to other studies of CHP systems which have considered hourly [23,70], weekly or monthly temporal resolutions [40,50]. The GA Optimisation Toolbox within MATLAB R2015b is used throughout along with meteorological data and time series of both electrical and heating load profiles spanning a winter season (three months). This paper is organised as follows: Section 2 illustrates the methodology; Section 3 covers the results and discussion followed by the conclusions in Section 4 along with some recommendations for future research.

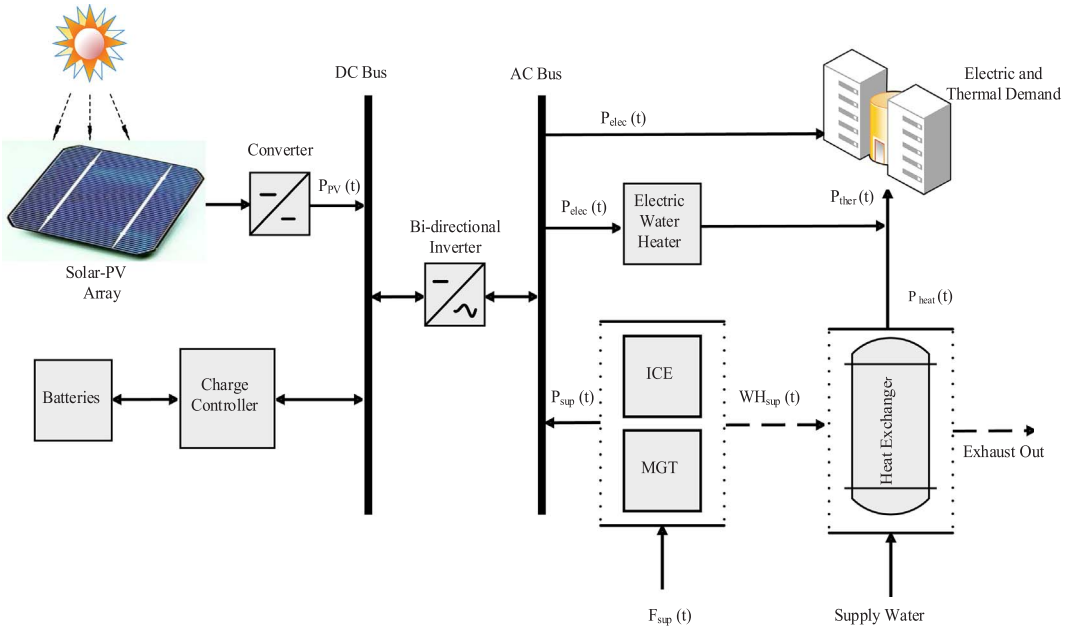

Fig. 1. Schematic diagram of stand-alone hybrid CHP system.

2. Methodology

The conceptual design architecture of the stand-alone hybrid co-generation system that is considered is shown in Fig. 1. The key hardware components are PV modules, supplementary prime movers in the form of multiple similar units of Internal Combustion Engines (ICEs) or Micro Gas Turbines (MGTs), batteries (Batt), Heat exchangers (Hex) and inverters. The system considered meets three relative magnitudes of highly dynamic load profiles which have been processed so as to vary their relative magnitudes but retain their time fluctuating nature. The first is designated as 60:40 shown in Fig. 2(a). The mean for the electric load demand is 28.88 kW and the standard deviation is 29.53 kW; the mean for the thermal load is 17.95 kW and the standard deviation is 49.44 kW. The second load profile is designated as 40:60 shown in Fig. 2(b), where the thermal demand exceeds the electric. In this regard, the mean for the electric load demand is 17.95 kW and the standard deviation is 18.35 kW; the mean for the thermal load is 28.88 kW and the standard deviation is 56.26 kW. This research also considers a third load profile as 30:70 shown in Fig. 2(c). The mean for the electric load demand is 13.46 kW and the standard deviation is 13.76 kW; the mean for the thermal load is 33.69 kW and the standard deviation is 65.64 kW. Our earlier work [65] has featured a similar electric load profile but of a lower overall magnitude and modelled in the context of stand-alone systems that have no waste heat recovery or the need to meet a thermal demand as in the present study.

2.1. PV model and meteorological data

In order to determine the time resolved solar power generation, the performance characteristics curve of commercially available PV modules is used (Make: Heckert Solar, Model: HS-PL 135) [71]. These are mono-crystalline silicon PV modules of 0.8 m^2 and 135 W each, maximum power point voltage of 18 V, maximum power point current of 7.48 A, nominal open circuit voltage of 22.3 V, and a short circuit current of 7.95 A [71,72]. Dynamic profiles of solar irradiation data and ambient temperature, both shown in Fig. 3, are used in the simulations. These are for a remote location in Western Australia and obtained from the Australian Bureau of Meteorology (Broome: latitude: 17°56′S, longitude: 122°14′E) [73]. The total annual availability of solar irradiance is 2290 kW/m^2, with a peak of 1.14 kW/m^2. The performance of the PV modules at any time interval is dependent on the cell temperature, which itself a function of solar irradiation, ambient temperature, and wind speed, all of which have not been commonly integrated in many previous studies when deriving PV power [59,74,75]. In this study, a mathematical model based on a single diode equivalent circuit for PV modules, wherein the effects of ambient temperature and wind speed on the power output have been used [76,77]. The PV module parameters such as the light current, diode reverse saturation current, series resistance, shunt resistance, and the modified ideality factor are calculated to determine the solar current. These parameters can be obtained using the *I-V* characteristics provided by the manufacturer at reference conditions and other known hardware specific characteristics [71]. As such, this study also includes a detailed modelling of the renewable power generated using methods found in the Appendix D. In this study, Renewable Penetration (RP) is percentile which expresses usable PV energy converted to meet load but excludes dumped/excess energy relative to the load demand, made of electric P_{elec} (t) and thermal P_{ther} (t) at any time step.

2.2. Battery modelling

In this study, the primary role of the battery bank is to supply the necessary energy if PV is unable to satisfy part of the load demand (electric and thermal) or if the minimum starting threshold ($P_{sup,min}$) of supplementary prime movers is not reached to warrant their operation. As such, batteries are not used for seasonal (bulk) energy storage. Surplus energy generated by the PV modules is stored in the batteries and redrawn from the battery when required. After meeting the thermal demand P_{ther} (t) in any time interval, excess energy from supplementary prime movers is also used to charge the battery bank. Lead acid batteries of 200 A h nominal capacity, 12 V nominal voltage, and round-trip efficiency of 85% have been considered [78]. For the longevity of the battery bank, the battery should not be overcharged or over-discharged. The maximum charge ($B_{SOC,max}$) is set to the nominal capacity of each battery and the minimum state of charge is represented by $B_{SOC,min} = 0.2B_{SOC,max}$ for longer battery life [57]. In the simulations, the battery charge efficiency is taken equal to the round trip efficiency, whereas the discharge efficiency is 100% [57]. The battery charging and discharging equations are adopted from Appendix E. The battery bank is connected to the PV modules through a charge controller. The DC and AC buses are connected by the bi-directional inverter which converts DC voltage (from PV and battery sources) to AC voltage to supply AC loads, and alternatively AC voltage (from prime movers) to DC voltage to charge the battery bank. The conversion efficiency of the bio-directional inverter is considered as 95% [79].

2.3. Supplementary prime movers

The conceptual CHP systems considered in this study integrates one or more units of similar combustion-based prime movers to supplement the PV/Batt and meet the electric demand. These supplementary prime movers are either Internal Combustion Engines (30 kW ICE) or comparable rating Micro Gas Turbines (30 kW MGT). An exhaust heat recovery system is coupled with the ICE or MGT units so as to meet

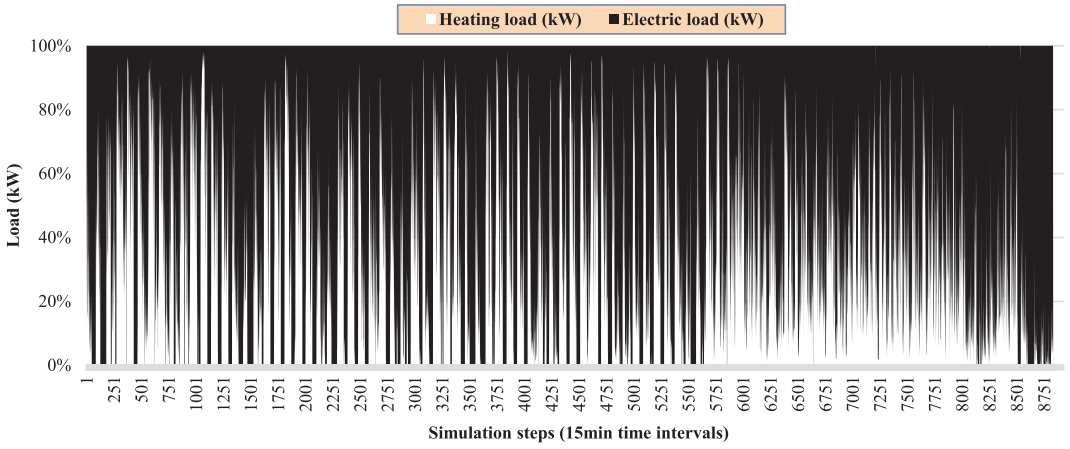

Fig. 2a. Electricity (64,462 kW h) and heating (40,058 kW h) load demand (60:40) of the selected area.

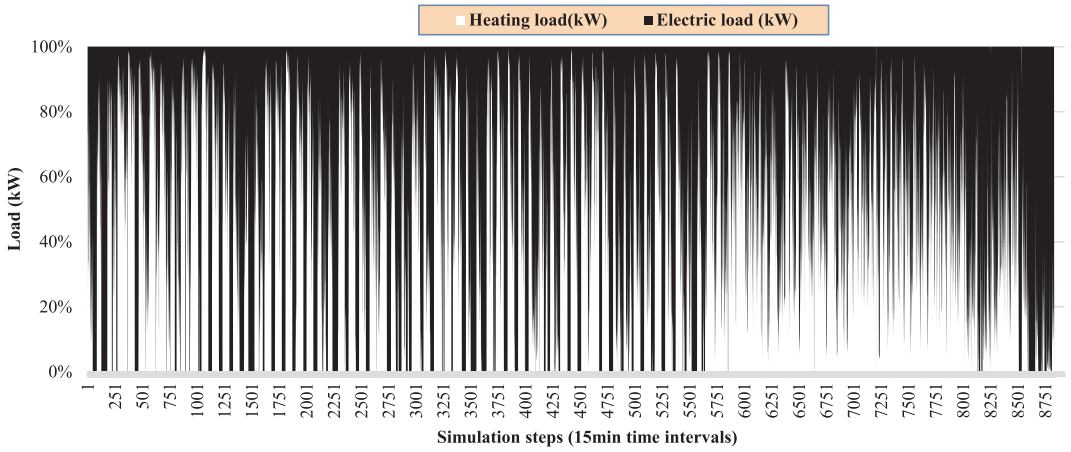

Fig. 2b. Electricity (40,058 kW h) and heating (64,462 kW h) load demand (40:60) of the selected area.

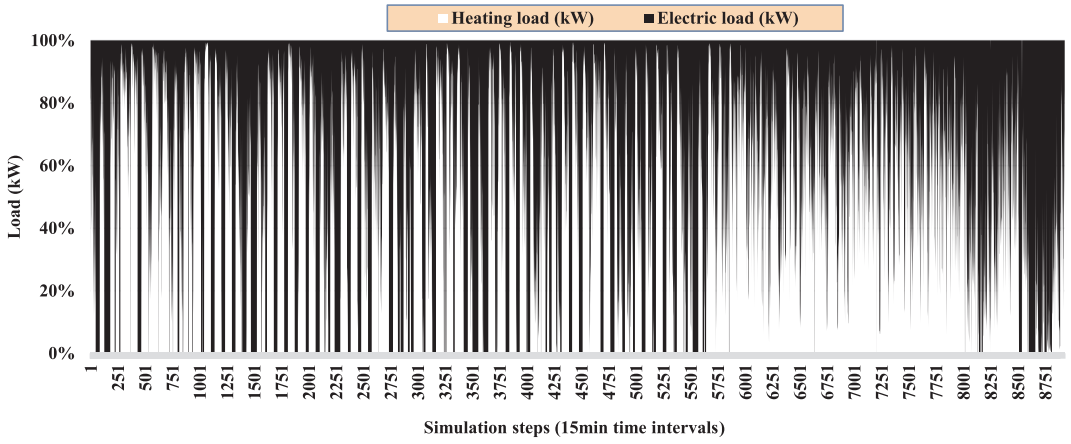

Fig. 2c. Electricity (30,050 kW h) and heating (74,470 kW h) load demand (30:70) of the selected area.

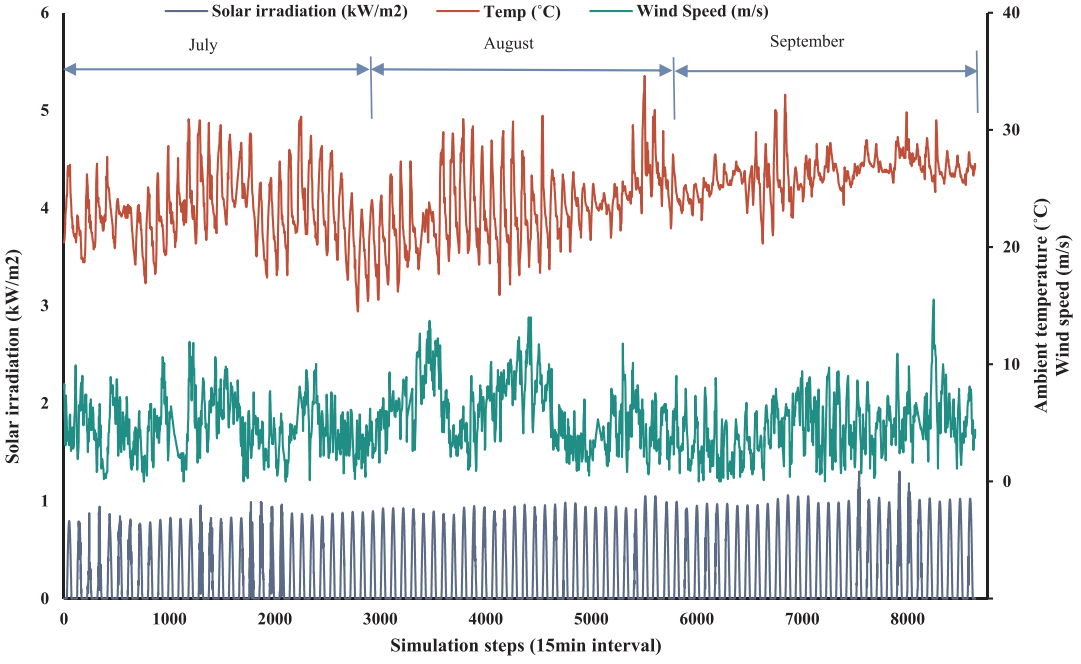

Fig. 3. Time resolved solar irradiation, ambient temperature, and wind speed over three months (July to September 2016).

thermal demand. The performance characteristics of commercially available ICEs and MGTs are chosen for system modelling [80,81]. The fuel energy (F_{sup} (t)) supplied to each supplementary prime mover corresponds to the output power (P_{sup}) of these prime movers in every time step based on their instantaneous thermal efficiency (ICE: 33–37% over 10 kW–30 kW; MGT: 20.6–26% over 10 kW–30 kW). It is assumed that all simulation parameters remain constant during each time interval. A minimum time step of 15 min has been considered in this study. The relatively small temporal resolution used allows for sensitivity to any higher frequency of prime mover start/stops as well as partial load operation, both of which can cause significant amounts of fuel consumption and long term maintenance problems [82,83]. In any time steps, the fuel consumption rate (kg/h) for the 30 kW ICE and the MGT are derived using the polynomial fits of engine operating characteristics (Eqs. (1) and (2), respectively) [80,81,84], where $P_{ICE}(t)$ and $P_{MGT}(t)$ is the power generation from the ICE and MGT, respectively. The ambient temperature is also used to model MGT to calculate the output power. Fig. 4 represents the normalised performance characteristics curves for the 30 kW ICE and the MGT.

$$C_{fuel,ICE,30}(t) = 0.0001 \times P_{ICE}^2(t) + 0.2108 \times P_{ICE}(t) + 0.3551 \quad (1)$$

$$C_{fuel,MGT,30}(t) = 0.00005 \times P_{MGT}^2(t) + 0.3132 \times P_{MGT}(t) + 0.7054 \quad (2)$$

In this regard, consumed fuel energy (kW) can be determined using Eq. (3), where LHV is the lower heating value of the fuel (43,100 kJ/kg for diesel in the ICE and 43,250 kJ/kg for natural gas in the MGT).

$$F_{sup}(t) = \frac{C_{fuel,sup}(t) \times LHV}{3600} \quad (3)$$

In this study, a Thermal to Electric Ratio (TER) is determined from Eq. (4), where Q_{th} is the recoverable heating energy. Systems have higher TER for MGT (typically 1.37–2.17) as compared to ICE (0.84–1.96) that implies comparatively more heat generation [84].

$$TER = \frac{Q_{th}(t)}{P_{sup}(t)} \quad (4)$$

The recoverable heating energy ($Q_{th}(t)$) includes the combined waste heat of exhaust gas and jacket water for the ICE, but only waste heat of exhaust gas for MGT which is air cooled. In this paper, a TER value of 2.17 for the MGT and 1.96 for the ICE has been considered for calculating the potential to meet a thermal load in each time interval. Additionally, the Recovered Waste Heat to Power Generation (RWHP) is defined by the Eq. (5), where $P_{heat}(t)$ is the thermal load met by the recoverable heating energy ($Q_{th}(t)$) relative to the total (electric) power output (P_{sup} (t)) of the ICE or MGT over each time step.

$$RWHP = \frac{P_{heat}(t)}{P_{sup}(t)} \quad (5)$$

The consequential total life cycle emissions (LCE) are the sum of the emissions by the system components over their lifetime (cradle to grave) and includes that from fuel consumption. This is expressed by Eq. (6) [4], where, β_i (kg CO_2-eq/kW h) is the lifetime equivalent CO_2 emissions of each hardware component (i) and E_L (kW h) is the amount of energy converted (or stored in batteries).

$$LCE = \sum_{i=1}^{N} \beta_i E_L \quad (6)$$

2.4. Electric water heater

In this study, when the load deficit (P_{Net}) is below the minimum starting threshold of supplementary prime movers, process heating using electric resistance heaters (powered by renewables and batteries) is used to supply the necessary heating load. The electric energy (kW h) requirements can be measured from the overall process heater efficiency ($\eta_{wh,sys}$) which is calculated by the Eq. (7) [85], where E_{elec} is the electrical energy input to the heater and E_{ther} is the total thermal energy. In this study, an efficiency, $\eta_{wh,sys}$ = 97% has been considered for system modelling [86]. In the present study, the thermal load is composed purely of heating (no cooling as with CCHP).

$$\eta_{wh,sys} = \frac{E_{ther}(t)}{E_{elec}(t)} \quad (7)$$

2.5. Load profile and reliability index

The Loss of Power Supply Probability (LPSP) is extensively used as a reliability index for sizing hybrid power generation when meeting electric loads [56–59]. However, the LPSP has not been considered while meeting thermal demand [51,60–65]. In this regard, the

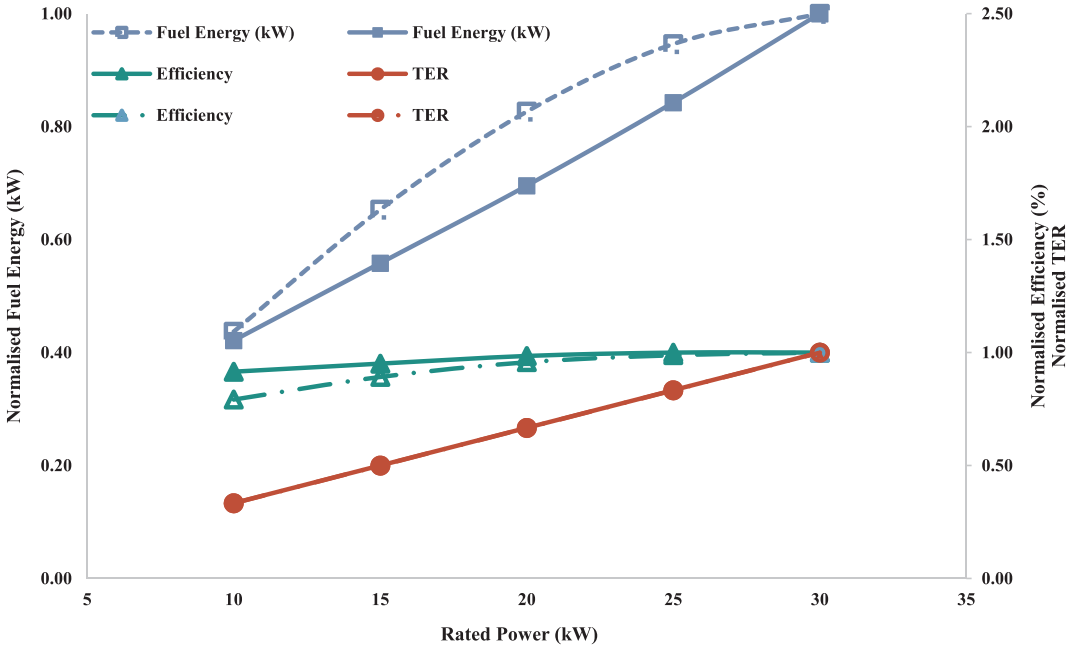

Fig. 4. Normalised fuel energy, efficiency, and Thermal to Electric Ratio (TER) of a typical 30 kW ICE (solid) and MGT (dashed).

simulations within this paper consider a combined electric and thermal load when deriving the optimum system. The target reliability is based on the LPSP (combined electrical and thermal) and is calculated using Eq. (8), where by $LPS_{elec}(t)$ and $LPS_{ther}(t)$ are the missed (kW h) electric and thermal in any time interval and $E_{elec}(t)$ and $E_{ther}(t)$ are the total electric and thermal load demands, respectively, over the period (T). It should be noted here that in order to modify the expression for LPSP from that applied to electric loads [59], two terms (for thermal load) have been introduced into the numerator and denominator of Eq. (8). In the present paper, t = 15 min and T = 132,480 min (8929 time steps, 3 months).

$$LPSP = \frac{\sum_{t=1}^{T}(LPS_{elec}(t) + LPS_{ther}(t))}{\sum_{t=1}^{T}(E_{elec}(t) + E_{ther}(t))} \quad (8)$$

where, $LPS(t) = (LPS_{elec}(t) + LPS_{ther}(t))$ (9)

In this case, the LPS (t) can be calculated using the following equation (modified from the electric loads [59]):

$$LPS(t) = (P_L(t) - P_{sup}(t) - P_{heat}(t)) \times \Delta t - (P_{PV}(t) \times \Delta t + \frac{C_b}{\Delta t} \times (B_{SOC}(t-1) - B_{SOC,\min})) \times \eta_{inv} \quad (10)$$

Any time interval, the total load P_L (t) is designated to be the sum of the electrical load P_{elec} (t) and the thermal load P_{ther} (t). Fig. 2 represents the electric load and heating load demand for both 60:40, 40:60, and 30:70 load profiles. The maximum value of the LPSP constraint is taken as 0.01 ± 0.005, which is equivalent to a missed load of 1045 kW h combined electric and heating.

2.6. Power management strategy

In this study, the hybrid cogeneration system is assumed to meet a time varying domestic hot water supply and electric load as represented by a specific (combined) LPSP. A Power Management Strategy (PMS) is the switching algorithm which controls various components and is given in Fig. B.1 (Appendix B). This study includes a comparison between two types of PMS. The first is a strategy which sets operating decisions based on meeting the electric load and then using the consequential waste heat from supplementary prime movers to satisfy part/all the heating load (termed FEL). The second strategy is hybrid (termed FEL/FTL) and necessarily meets both the electric and heating loads.

Power generated from the PV module P_{PV} (t) is compared with P_L (t) to determine the net deficit P_{Net} (t) = P_{PV} (t) - P_L (t) in each time interval. The deficit P_{Net} (t) can either be met solely by renewables, requires augmentation through discharging battery storage at P_B (t), or operating supplementary prime movers at P_{sup} (t). Below the minimum starting threshold ($P_{sup,min}$) of supplementary prime movers which is set at 30% of nominal rated power [87,88], PV along with the battery bank would supply necessary energy requirements. Where renewables are greater than the load demand (P_{Net} (t) > 0) but batteries are not fully charged (B_{SOC} (t) < $B_{SOC,max}$), surplus PV power is delivered to charge

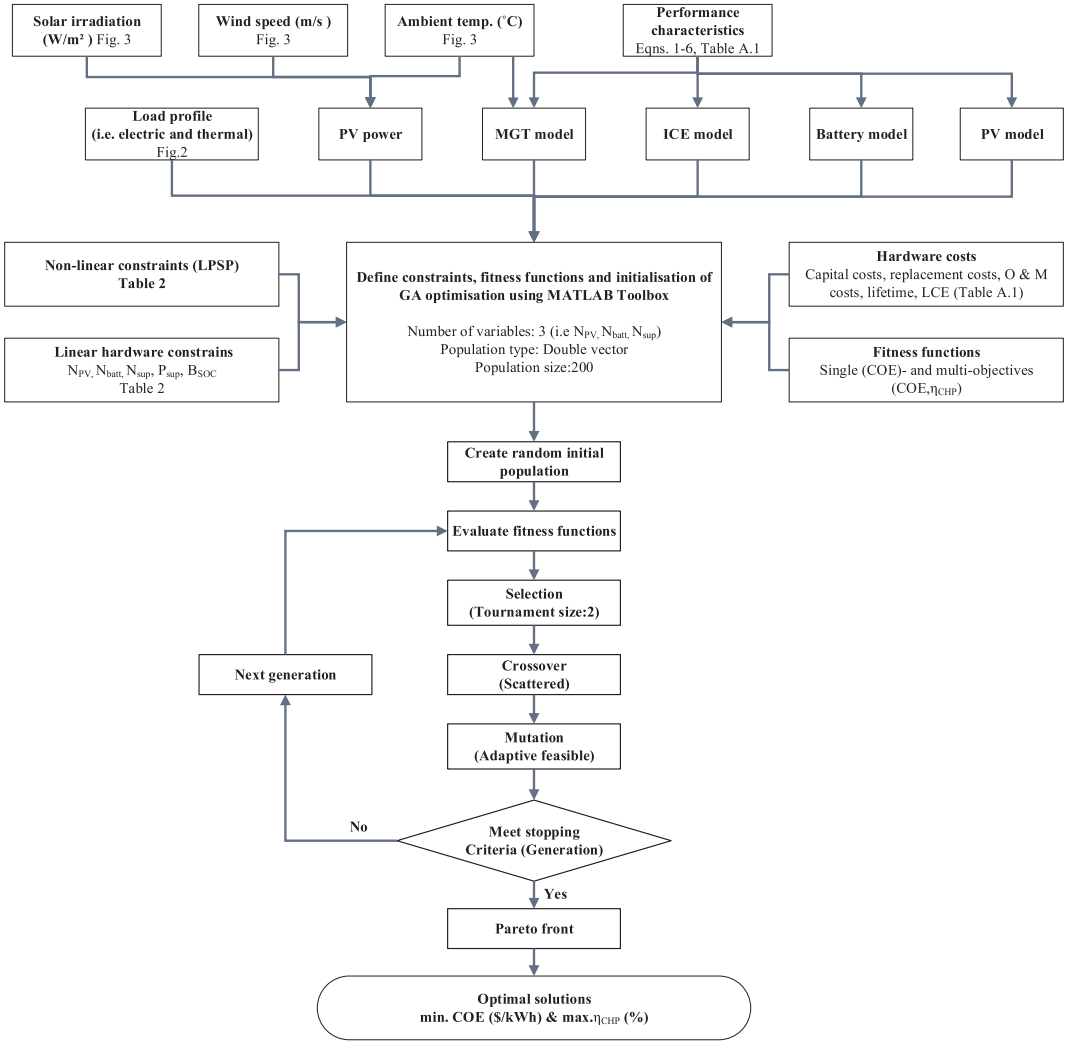

Fig. 5. Multi-objective GA procedure.

the battery bank at P_B (t). Once the battery state of charge reaches its maximum value ($B_{SOC,\ max}$), additional surplus power in this time interval is considered as excess energy EE (t) and dumped. Alternatively, when power generation from PV is equal the load demand P_{Net} (t) = 0, the load is met in that time interval (Meet P_L (t)). However, when the load demand is greater than renewables P_{Net} (t) < 0, but sufficient storage capacity exists (B_{SOC} (t) > $B_{SOC,min}$) and total energy (PV + Batt) is equal or greater than the demand, the battery would supply the necessary load demand alongside the PV. As soon as battery state of charge reaches its minimum level (B_{SOC} (t) = $B_{SOC,min}$), the deficit load requirement is considered as unmet (Unmet P_L (t)).

If P_{Net} (t) exceeds the minimum starting threshold for the prime movers ($P_{sup,min} \leqslant |P_{Net}(t)|$), the ICE or MGT are used to meet the demand (P_L (t)) when renewable energy along with battery bank is insufficient. At this stage, the prime movers are operated to meet all the electricity demand (P_{elec} (t)) and the thermal demand (P_{ther} (t)) using the waste heat recovery system. However, for a hybridised system such as that described in this study, when the heating load is much higher compared to the electrical demand, prime movers only can meet part of the thermal demand. In such time intervals, the PMS shifts from FEL to FEL/FTL where prime movers supplement power to first meet the relatively higher heating load requirements. In Fig. B1 (Appendix B), this strategy is shown using a dashed box, where the supplementary prime mover switches priority so as to meet the thermal demand P_{ther} (t) instead of P_{elec} (t). The PMS then checks whether it also meets the electric demand in that same time interval. In this regard, the deficit (combined) electric and heating load requirements are considered as Unmet P_L (t). On the other hand, the additional electric energy generated by the ICE or MGT, after meeting the demand, is used to charge batteries until they reach their maximum state of charge ($B_{SOC,\ max}$), with the excess being dumped. In an FEL strategy, after first meeting electricity demand (P_{elec} (t)), the recovered waste is used to meet the thermal demand (full P_{ther} (t) or part of it). The rest of the heating demand is met by the electric (resistance) water heater if there is enough state of charge (> $B_{SOC,\ min}$) or it is considered as (Unmet P_L (t)). In this study, for both cases (i.e. FEL/FTL and FEL) if the P_{elec} (t) load is below the minimum starting threshold of the supplementary prime mover, the electric demand (P_{elec} (t)) is then met by the PV and battery bank, whereas the thermal demand (P_{ther} (t)) is met by the electric resistance heating operated using PV along with a battery bank.

2.7. GA optimisation, modelling parameters, and constraints

In this work, at first the system is optimised based on single objective function (COE, $/kW h) using a MATLAB-based Genetic Algorithm (GA). The results obtained from single objective optimisation are then compared with the multi-objective optimisation technique using the same modelling parameters and constraints. The solution of a multi-objective optimisation problem, such as that in the present paper, may yield a set of non-dominant solutions known as Pareto optimal solutions. In arriving at these solutions, the simulations solve for a number of objective functions subjected to inequality constraints (LPSP in this study). The optimisation process search's for optimum values that are to be maximised (or minimised) for the objective functions subject to bounds (limits). System sizing can be formulated as follows [89,90]:

$$\left.\begin{array}{lll} Min/Max & F(x) = [f_1(x), f_2(x), f_3(x), & \ldots \ldots\ldots, f_n(x)] \\ Subject\ to & G_j(x) \leqslant 0 & j = 1,2,\ldots\ldots\ldots,J \\ & H_k(x) \leqslant 0 & k = 1,2,\ldots\ldots\ldots,K \end{array}\right\} \quad (11)$$

In this context, F is the expression for the objective function (either singular or multiple), x are the decision variables, G are the inequality constraints (e.g. LPSP), and H are the equality constraints (e.g. B_{SOC}, P_{sup}). In this study, multi-objective Genetic Algorithm optimisation problems have two objectives over the span of the period modelled (three months): the COE is to be minimised while the energy efficiency η_{CHP} of combustion based supplementary prime movers is maximised. Alternatively, single objective optimisations are solely based on the COE, albeit with the resulting (consequential) η_{CHP} also reported in the results given. The sizing optimisation using multi-objective Genetic Algorithm is summarised in Fig. 5. A summary of other studies and parameters used in other single- and multi-objective optimisation of CHP systems is shown in Table 1. The technical and economical details of the hybridised system components are incorporated to the fitness function and the constraints (i.e. linear and non-linear constraints). These are defined as an input to the optimisation toolbox. Additionally, a set of parameters need to be specified before the optimisation process running such as population type and size, selection function, crossover function, mutation function, and stopping criteria. In this regard, the selection function is chosen as tournament with size 2, crossover function is the scattered, and mutation is the adaptive feasible as there is both linear and non-linear constraints. The stopping criteria is selected based on the specified number of generations (100 in this study) and the function tolerance is $1e^{-6}$. Using the given input parameters, multi-objective GA optimisation offers an iterative process until the

Table 2
Optimisation constraints.

Decision variables	Lower bound	Upper bound
N_{PV}	100	1000
N_{batt}	10	50
N_{sup}	1	10
B_{SOC}	20	100
P_{sup}	0	30
LPSP	0.005	0.015

Table 1
GA application for optimisation of CHP systems.

System components	No of objectives	Modelling parameters	Optimisation parameters
PV + MGT/ICE [39]	Single	COE, emissions	Population size 50, number of generation 80, crossover probability 0.8, mutation factor 0.2, selection function Roulette, crossover function arithmetic
Gas turbine + solar thermal plant [93]	Multi	Exergy analysis, product cost	Population size 350, number of generation 3500, crossover probability 0.4, selection process tournament, mutation function constraint dependant
ORC + HRSG [94]	Multi	Exergy efficiency, overall capital cost	Population size 30, number of generation 150, crossover probability 0.7, selection process tournament
Gas turbine + ORC + HRSG + Absorption chiller + PEM [95]	Multi	Exergy efficiency, total cost rate	Population size 100, number of generation 250, crossover probability 0.9
Gas turbine + ORC + HRSG [96]	Multi	Thermal efficiency, total volume of the system, and net present value	Population size 1000, number of generation 200, crossover probability 0.8, selection process tournament

Table 3
Summary results of single (COE) and multi-objective (COE and η_{CHP}) optimisations of hybrid CHP systems (load profile 60:40, LPSP = 0.01 ± 0.005).

Characteristics	PV/Batt/ICE				PV/Batt/MGT			
	Single objective		Multi-objective		Single objective		Multi-objective	
	FEL/FTL	FEL	FEL/FTL	FEL	FEL/FTL	FEL	FEL/FTL	FEL
Number of solar panels, N_{PV}	976	922	968	974	967	959	780	973
Number of lead acid batteries, N_{batt}	42	50	25	44	32	43	15	37
Number of prime movers, N_{sup}	2	2	2	1	1	1	1	1
$LPSP_{comp}$	0	0.0111	0	0.0077	0.0009	0.0085	0.0096	0.0079
PV energy generated (kW h)	62,573	59,111	62,060	62,444	61,355	61,483	50,007	62,380
Renewable penetration, RP (%)	60	57	59	60	59	59	48	60
ICE/MGT energy, P_{sup} (kW h)	25,724	33,453	27,602	32,265	27,398	33,105	35,318	33,393
RWHP (%)	76	35	77	35	78	37	72	37
Unmet energy (kW h)	0	1165	0	802	99	885	1008	826
Fuel energy, F_{sup} (kW h)	69,139	90,824	74,203	87,588	110,090	132,130	142,630	133,280
Recovered waste heat to thermal demand (P_{heat}/P_{ther}, %)	49	29	53	28	53	30	63	31

predefined stopping criteria is met. In the process of optimisation, each generation calculates the LPSP for each population member. For those cannot satisfy the load requirements of a certain value of LPSP is excluded from the population for next generation to progress crossover, migration, and mutation processes. The process continues until all generations are finished. Finally, the Pareto front is selected which gives the values of all non-inferior solutions. More details about the methodologies of multi-objective Genetic Algorithms can be found in literature [89,91] and from the Help menu in the MATLAB optimisation Toolbox.

The overall efficiency of supplementary prime mover-based cogeneration systems is determined from Eq. (12), where P_{heat} (t) is the heating load demand met using the waste heat recovered from the ICE or MGT:

$$\eta_{CHP}(t) = \frac{P_{sup}(t) + P_{heat}(t)}{F_{sup}(t)} \tag{12}$$

In this study, the COE can be calculated using Eq. (13), where C_A is the total annualised energy system cost which includes: capital costs, Operation and Maintenance (O & M) costs, discount rate and fuel costs of system components. The discount rate for energy generation projects differs from 5% to 10% [92]. In this paper, a value of 10% is considered with a project lifetime of 25 years in accordance with maximum lifetime of PV module. Additionally, E_s (kW h) is the annual load to be met (electrical and thermal). Further details in this regard are given in [87].

$$COE = \frac{C_A}{E_s} \tag{13}$$

The annualised cost is sum of annualised capital cost ($C_{A,cap}$), annualised Operation and Maintenance cost ($C_{A,O\&M}$), and annualised fuel cost ($C_{A_{fuel}}$) of the system components and can be calculated by the Eq. (14),

$$C_A = C_{A,cap} + C_{A,O\&M} + C_{A,fuel} \tag{14}$$

The data for cost and equivalent CO_2 emissions attributed to the system components are presented in the Appendix A (Table A.1). Cost's presented represent only hardware and do not include civil works, mechanical, and electrical fabrication works as well as installation and labour costs. However, the cost associated with the heat recovery system does include with the capital cost of a 30 kW MGT. The cost for circulation pumps, interconnection piping, and control instrumentation are not considered in this study.

The study utilises MATLAB optimisation toolbox to implement the single- and multi-objective genetic algorithm. In this regard, the nonlinear constrains (representing the calculation of LPSP) are written in one M-file, whilst another M-file representing the fitness function (using the PMS, and Eqs. (12) and (13)) calculates the all objective functions. The decision variables considered in this optimisation are the number of PV modules N_{PV}, the number of lead acid batteries N_{batt}, and the number of supplementary prime movers N_{sup}. The simulations are also subjected to some constrains presented in Table 2 which are initially determined using trial and error to ensure the target LPSP (0.01 ± 0.005) is satisfied. Constraints B_{SOC}, P_{sup}, and LPSP are formulated in the PMS, and other constrains related to bounds (number of components, N_{PV}, N_{batt}, N_{sup}) are directly entered into the optimisation toolbox. In achieving these simulations, a sensitivity analysis is also done into the effects of population size on the solutions in both single- (COE) and multi-objective (COE, η_{CHP}) optimisations. Fig. C1 (Appendix C) shows that with single objective optimisation, a population size of 10 is chosen as no appreciable improvement in the COE is achieved with further increases in the population size (up to 50), albeit it at the expense of computational time. In the case of multi-objective optimisations, although a larger population size is needed, both the COE and the η_{CHP} stabilise for a population size of 200. Additionally, in single objective optimisations, constraint dependent mutations, a crossover fraction of 0.8 with scattered function, elite count 2, and 50 generations are used. On the other hand, a crossover fraction of 0.8 with 100 generations are used in the MATLAB multi-objective optimisation toolbox.

3. Results and discussion

The data which follows examines the effects of two types of PMS, the more commonly used type governing device switching based only on electric load demand (FEL), and a hybrid PMS which accommodates following both electric and thermal loads which are made up completely of heating in this study (FEL/FTL). The results will also discuss how changes to the relative proportions of electric to thermal load affect the optimisation of a hybrid CHP system over one season (3 months). Most of the analyses presented are based on single objective optimisation (COE, $/kW h) but the sensitivity of the outcomes to alternatively using a multi-objective function optimisation (COE, $/kW h; η_{CHP}, %) is also given.

3.1. Type of load following strategy

The first set of results presented considers prime movers having $P_{sup,min}$ = 30% whereby the Electric to Thermal Load Ratio (ETLR) is 60:40. Summary data are presented in Table 3, with the first three rows giving the optimised size (i.e., the solution to the system's sizing

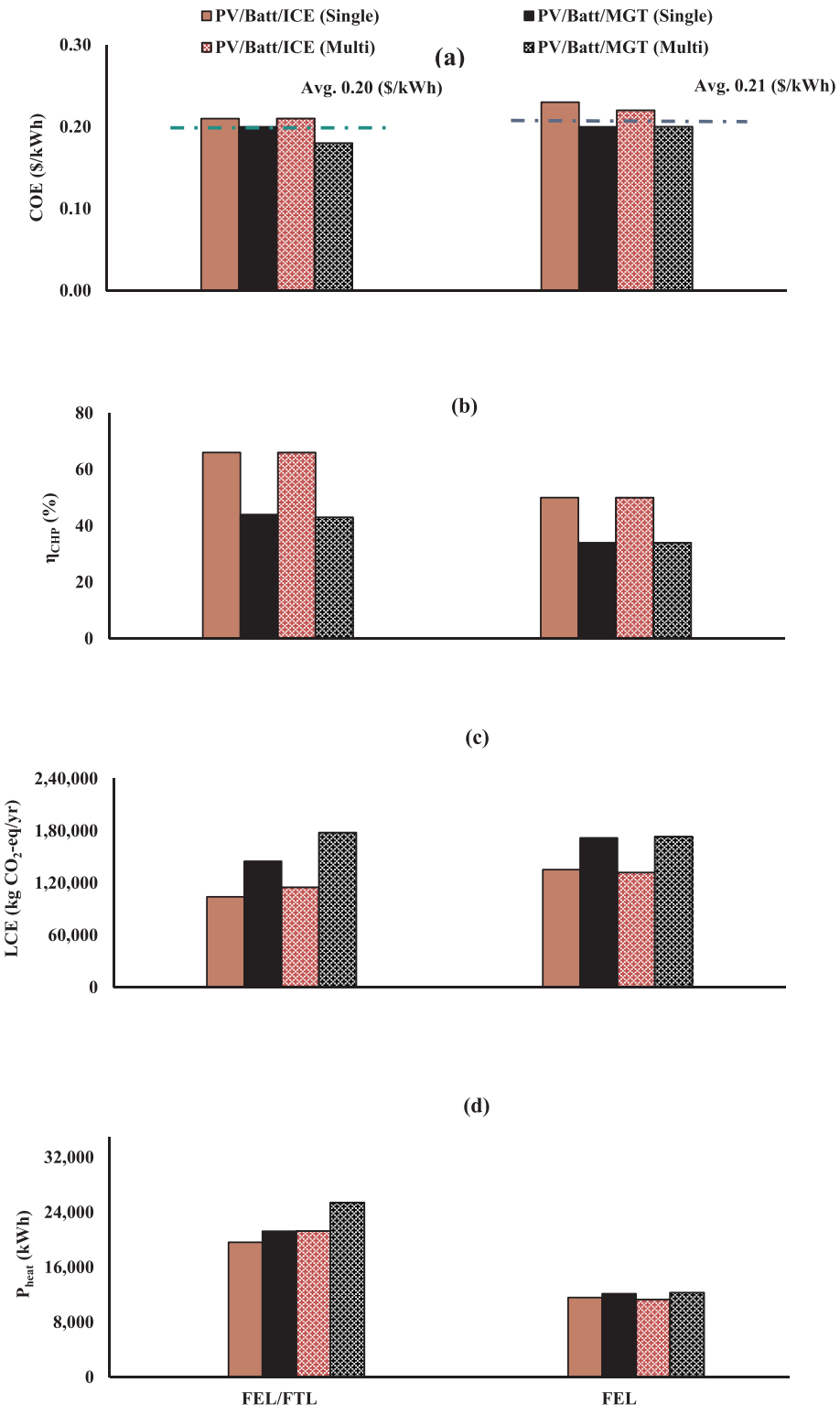

Fig. 6. The effects of load following strategy (FEL/FTL, FEL) on hybrid CHP systems operating to meet load profiles with an ETLR = 60:40. A comparison between single- (COE) and multi-objective optimisations (COE, η_{CHP}) are shown for both PV/Batt/ICE and PV/Batt/MGT.

problem) and the remaining rows identifying the consequential performance.

From Fig. 6(a) it is evident that a PMS based on FEL/FTL or FEL has comparable COE whether optimised using single- or multi-objectives. For PV/Batt/MGT-based systems, PMS hybridisation (FEL/FTL) has an insignificant effect on the COE (avg. 0.19$/kW h) compared to FEL (avg. 0.20$/kW h). Similarly, for PV/Batt/ICE-based systems, PMS hybridisation only marginally gives better COE (avg. 0.21$/kW h) compared to FEL (avg. 0.23$/kW h). It is also evident from the results that the COE for the PV/Batt/MGT is generally (slightly) lower in contrast to PV/Batt/ICE systems. The COE for the PV/Batt/MGT is optimised as 0.27$/kW h in the literature [39]. This is attributed to the higher RWHP with PV/Batt/MGT systems, the lower price of natural gas used to run MGT's (3.3$/GJ) compared to diesel (0.91$/l).

Table 4
Summary results of single objective (COE, $/kW h) optimisations of hybrid CHP systems operating at different ETLR (P_{elec}:P_{ther}) for hybrid CHP systems (LPSP = 0.01 ± 0.005, $P_{sup,min}$ = 9 kW).

System characteristics	PV/Batt/ICE (FEL/FTL)			PV/Batt/MGT (FEL/FTL)		
	(60:40)	(40:60)	(30:70)	(60:40)	(40:60)	(30:70)
Number of solar panels, N_{PV}	976	864	989	967	979	994
Number of lead acid batteries, N_{batt}	42	48	50	32	50	50
Number of prime movers, N_{sup}	2	7	7	1	4	4
$LPSP_{comp}$	0	0.0530	0.0957	0.0009	0.0414	0.0993
PV energy generated (kW h)	62,573	55,392	63,406	61,355	62,765	63,727
Renewable penetration, RP (%)	60	53	60	59	60	61
ICE/MGT energy, P_{sup} (kW h)	25,724	24,981	18,694	27,398	22,670	18,956
RWHP (%)	76	97	115	78	99	115
Unmet energy (kW h)	0	5542	10,070	99	4327	10,453
Fuel energy, F_{sup} (kW h)	69,139	67,612	50,707	110,090	90,277	75,932
Recovered waste heat to thermal demand (P_{heat}/P_{ther}, %)	49	37	29	53	35	29

However, the higher capital cost of each MGT unit (Appendix, Table A1) also means optimisations always select fewer MGT units than ICE units as shown in Tables 3 and 4.

In relation to the Overall CHP Efficiency (η_{CHP},%), the FEL/FTL PMS in both single- and multi-objective optimisations is better than the FEL PMS. Optimisations when applied to size the ICE-based systems on FEL/FTL give η_{CHP} = 66% for both single- and multi-objective optimisations as shown in Fig. 6(b). However, in the case of ICE-based systems using an FEL, the overall efficiencies are much lower at η_{CHP} = 50% for both single- and multi-objective optimisation. In MGT-based systems running on a FEL/FTL PMS, η_{CHP} = 44% and η_{CHP} = 43% with single- and multi-objective optimisations. These also fall when alternatively operating on an FEL PMS for single- and multi-objective optimisations with η_{CHP} = 34%. From the above discussion, it is also evident that the η_{CHP} (%) for the ICE in the PV/Batt/ICE systems have higher η_{CHP} (%) than the PV/Batt/MGT system under the same operating conditions. The reason behind this is that the ICE has higher thermal efficiency (33–37% over 10 kW–30 kW) as compared to the MGT (20.6–26% over 10 kW–30 kW). The output power for an MGT is also more susceptible to ambient temperature changes (rated power is up to 18 °C but decreases by a further 20% at 35 °C) which imposes an additional change across seasons.

Although in the FEL/FTL PMS there are no significant gains in COE or η_{CHP} between using single- and multi-objective optimisations, the latter produce slightly higher LCE ($kgCO_2$-eq/yr) in both ICE and MGT-based systems. This is because in multi-objective optimisation achieving a higher η_{CHP} the Genetic Algorithm attempts to maximise utilisation of the recovered waste heat so as to meet the thermal demand, which attributed to relatively higher contributions from supplementary prime movers. Therefore, the number of PV modules and batteries are less in multi-objective solutions compared to the single objective optimisation as see in Table 3. However, hybridisation of the PMS using FEL/FTL in CHP systems not only to marginally improve the COE but more cleanly the η_{CHP}, it also carries some benefits in terms of LCE in both ICE and MGT systems. For example, the data in Fig. 6(c) shows that in ICE based CHP systems sized using single objectives, LCE = 135,340 $kgCO_2$-eq/yr with FEL but is smaller by around 30% at 104,010 $kgCO_2$-eq/yr with FEL/FTL. From Fig. 6(c) it is also obvious that the PV/Batt/ICE-based system produces lower LCE ($kgCO_2$-eq/yr) as compared to the PV/Batt/MGT-based system for similar following load and optimisation techniques. This is because of the higher lifetime equivalent CO_2 emissions (1.16$kgCO_2$-eq/kW h) for MGT than the ICE (0.88$kgCO_2$-eq/kW h).

In regard to the meeting thermal load demand using the recovered waste heat (P_{heat}), the multi-objective optimisation in the FEL/FTL mode is far higher than any other operating conditions as shown in Fig. 6(d). Table 3 shows that almost 50% of the thermal load demand is met by recovering waste heat from the supplementary prime movers while operating in the FEL/FTL mode for systems sized using single objective optimisation. This is even more (PV/Batt/ICE = 53%, and PV/Batt/MGT = 63%) while on the multi-objective optimisation for the same operating condition. On the other hand, only around 30% of the thermal demand is met by using the recovered heat when the system operating in the FEL mode regardless of optimisation technique (Table 3).

Despite this, the data also indicates the Renewable Penetration (RP) is comparable (57–60%) in both single- and multi-objective optimisations for the both FEL/FTL and FEL operating strategy except for PV/Batt/MGT system (48%) in multi-objective FEL/FTL mode. The reason behind this in multi-objective optimisation, the recovered waste heat to meet the thermal demand is higher (63%) than the other mode of operation and hence the optimisation select the fewer number of PV modules and battery bank to meet the load demand. However, in the FEL mode the PMS allows only to meet the thermal demand which is produced as a consequence of meeting electric demand first by the supplementary prime movers and the rest is met by the electric (resistance) water heater powered by the renewably charged battery bank. For this reason the number of battery is higher in FEL strategy than the FEL/FTL mode for all optimisation techniques.

From the above discussion, it is obvious that although the PV/Batt/ICE and PV/Batt/MGT hybridised CHP systems meeting a P_{elec} (t) and P_{ther} (t) have comparable COE, the overall CHP efficiency (η_{CHP},%) of the ICE is greater than that of the MGT regardless of optimisation technique under all operating conditions. The results also show that the FEL/FTL operating mode for both systems have higher share of meeting thermal demand using recovered waste and better environmental benefits than the FEL mode. This is true for both single- and multi-objective optimisation techniques. The renewable penetration is comparable for both systems in single-and multi-objective optimisation. Fig. 7 also shows that supplementary prime movers are responsible for meeting heating loads where these are relatively significant. The hybrid PMS therefore does not oversize the PV and battery capacities but relies on combustion engines.

3.2. Changes of Electric to Thermal Load Ratio (ETLR)

To analyse the effects of Electric to Thermal Load Ratio (ETLR) on the hybrid FEL/FTL strategy, Fig. 8 shows single objective optimisation data for ETLR = 60:40, 40:60, and 30:70. Results indicate that for PV/Batt/ICE systems, the effect of ETLR is very subtle on the COE (avg.

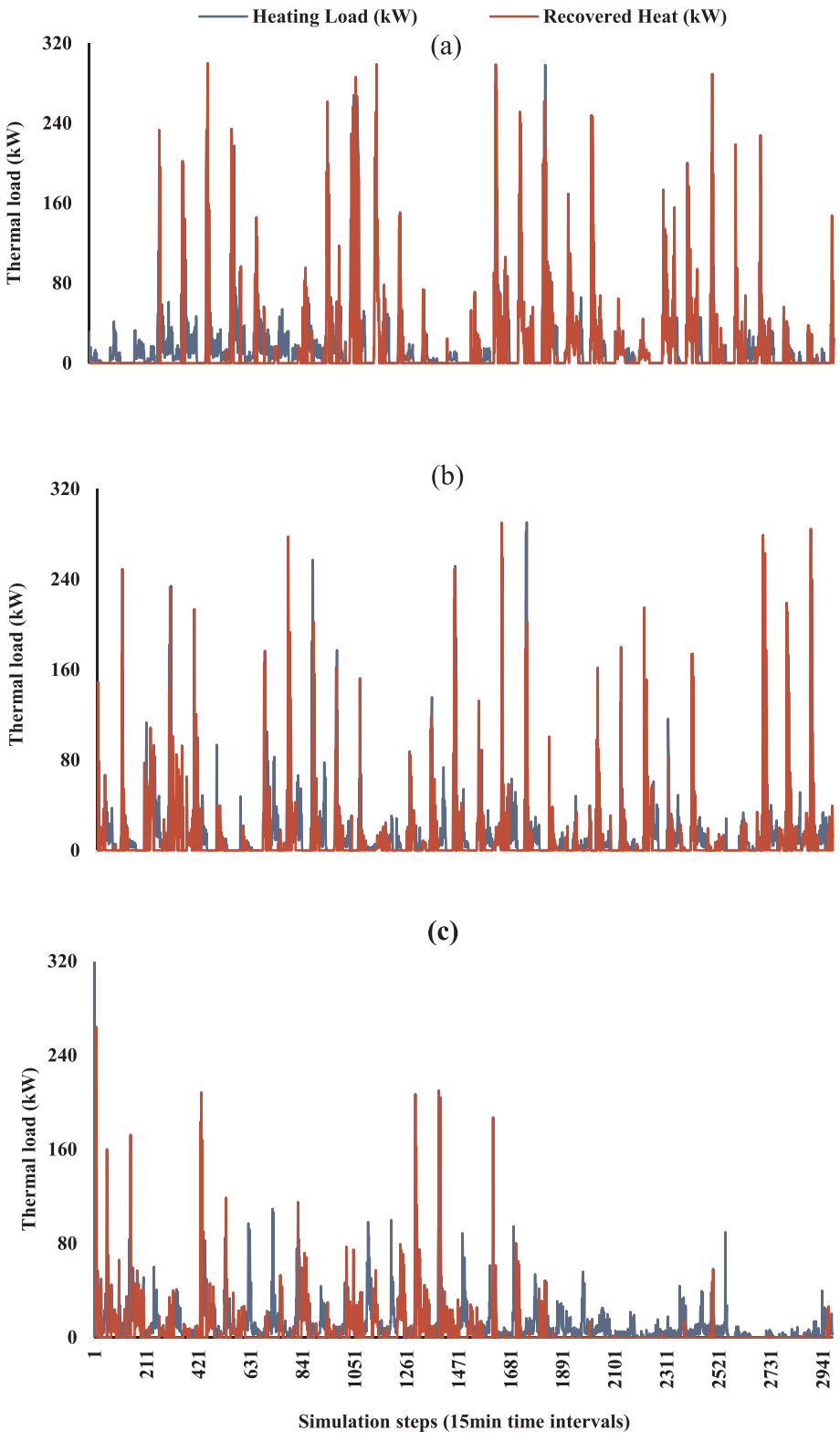

Fig. 7. Heating demand and recovered waste heat in (a) July, (b) August, and (c) September for PV/Batt/ICE in FEL/FTL PMS using multi-objective optimisation.

0.22$/kW h) in the case of ICE-based CHP systems. However with MGT-based CHP systems, increases to the relative significance of the thermal load (i.e. a smaller ETLR) generally lead to higher COE (0.20$/kW h for ETLR = 60:40, and ~ 0.30$/kW h for both ETLR = 40:60 and ETLR = 30:70). This is attributed to the fact that at lower electric load demand (P_{elec} (t)), as occurs with smaller ETLR, there is more likelihood of electric load falling below the minimum starting threshold ($P_{sup,min}$ = 9 kW) of supplementary prime movers at any time step. The PMS then forces the optimisation algorithm to select more PV modules and a larger battery bank irrespective of thermal demand in that time step. This also has the potential to cause a higher number of supplementary prime movers once the PV modules and battery units reach

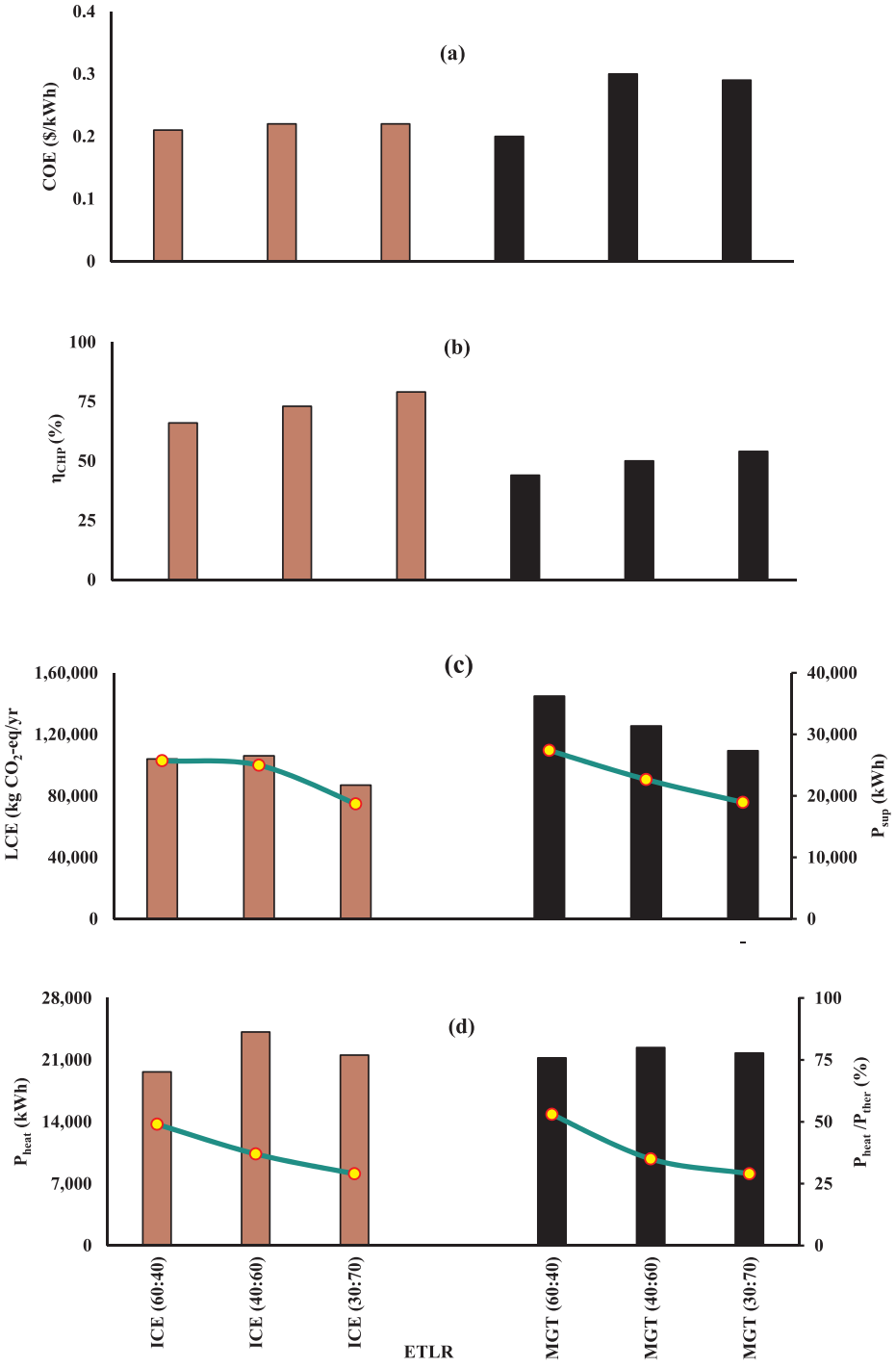

Fig. 8. The effects of Electric to Thermal Load Ratio (60:40, 40:60, and 30:70) on hybrid CHP systems sized using single objective optimisation in a PMS of the FEL/FTL type. Trend lines shown (figure c and d) should be read against the right vertical axis.

their upper bound in Table 2 to meet the specified LPSP (0.01 ± 0.005). The sizing data in Table 4 supports this. For the above reasons, at the greater thermal demand (e.g. ETLR = 30:70) the COE is higher. However, this is more apparent in PV/Batt/MGT systems as the capital unit cost of an MGT is higher than the ICE for the same power rating.

However, a more significant effect of ETLR appears in relation to the η_{CHP} (%) which increases significantly in the PV/Batt/ICE (from 66% at ETLR = 60:40 to 79% at ETLR = 30:70) when working on the FEL/FTL mode. This is because RWHP grows where there is greater thermal load than the electrical load. This change whilst still appreciable is less significant in the PV/Batt/MGT system (η_{CHP} = 44% at ETLR = 60:40 but 54% at ETLR = 30:70) which is attributed to the lower thermal efficiency of the MGT as compared to the ICE.

For hybrid systems operating with $P_{sup,min}$ = 9 kW in the FEL/FTL mode and meeting the same (combined) electrical and thermal demand, Fig. 8(c) shows that greater relative contributions of thermal load (from ETLR = 60:40 to ETLR = 30:70) lead to lower level of LCE. The LCE for the PV/Batt/ICE systems vary from 104,010 kgCO_2-eq/yr to 87,005 kgCO_2-eq/yr when the ETLR changes from 60:40 to 30:70. For the PV/

Batt/MGT systems, these vary from 144,900 $kgCO_2$-eq/yr to 109,380 $kgCO_2$-eq/yr when the ETLR changes from 60:40 to 30:70. This is because of the lower contribution of electric energy (P_{sup}) from the supplementary prime movers with bigger relative thermal contribution as shown in Fig. 8(c). The results also indicate that the PV/Batt/MGT produces more LCE ($kgCO_2$-eq/yr) than the PV/Batt/ICE for all operating conditions because of the MGT has the higher lifetime equivalent CO_2 emissions (Appendix, Table A.1). Although both the PV/Batt/ICE and the PV/Batt/MGT operating on the FEL/FTL mode have comparable recovered waste heat from the supplementary prime movers, the ratio of this recovered waste heat (P_{heat}) to the total thermal demand (P_{ther}) decreases significantly where there is larger thermal load as shown in Fig. 8(d).

In relation to renewable penetration, there are insignificant effects of changing the relative load profiles. From Table 4 it is evident that the reliability of meeting load demand (LPSP) decreases as ETLR changes from 60:40 to 30:70. This is due to more likelihood at smaller ETLR of electric loads falling below $P_{sup,min}$ in any time interval. This can lead to lower reliability (LPSP) since the GA optimisation algorithm cannot increase (PV, battery) units beyond the constraints set in Table 2.

4. Conclusions

Most research published to date on hybrid energy systems only considers following (meeting) an electric load. The present study has examined hybrid CHP systems and the effects of load following strategies (electric only versus electric and heating demand). Additionally, the relative magnitude of the thermal load has also been varied when determining the sizing optimisations so as to analyse the impact on COE, η_{CHP}, LCE, and other performance indicators. Genetic Algorithms based on single objective optimisations are used for system sizing with Loss of Power Supply Probability (LPSP) as the reliability index. The results are also analysed and compared to that of sizing CHP systems using multi-objective optimisations under the same constraints. Although the techno-economic feasibility and optimisation techniques presented in this study are based on a set of data and constraints and not intend to highlight the merits or limitations of certain types of prime movers (energy system components), the outcomes can be summarised as:

- **COE:** In CHP systems, the use of (solely) electric load following (PMS based on FEL) or both electric and thermal load following (FEL/FTL) has only marginal effects on the Cost of Energy (COE). Greater thermal loads relative to the total load to be met (i.e. a smaller ETLR) appear to have a stronger effect on the COE in MGT-based CHP systems.
- **η_{CHP}:** The more notable effect of PMS type in CHP systems appears in relation to the Overall CHP Efficiency (η_{CHP}). PMS hybridisation (FEL/FTL) results in better performance in both PV/Batt/ICE and PV/Batt/MGT systems, but particularly for ICE-based systems. A PMS based on FEL/FTL also allows for more thermal load to be satisfied using recovered waste heat (P_{heat}) when meeting the same load as a PMS based on FEL. In single objective optimisations, greater relative magnitudes of heating load demand also appear to lead to increased Overall CHP Efficiencies, with the degree of influence varying between ICE- and MGT-based CHP systems.
- **LCE:** Although using a PMS which follows both electric and thermal loads (FEL/FTL) in CHP systems does not carry with it significant financial incentives based on COE, it does however improve system Life Cycle Emissions (LCE) compared to an electric (only) load following strategy (FEL). The use of hybrid PMS in CHP systems (FEL/FTL) also leads to fewer LCE in system sized using single objective optimisations when the relative contributions of the thermal load increases (ETLR reduced).
- **Single- versus multi-objective optimisations:** One of the biggest merits from sizing CHP systems using multi-objectives (COE, η_{CHP}), compared to only using single objective (COE) optimisation, is to increase the fraction of total thermal demand which can be satisfied by recovered waste heat (P_{heat}/P_{ther}).

Whilst this research has focused on a hybrid stand-alone Combined Power and Heating (CHP) system, further research is warranted into systems taking into consideration a cooling load as well as heating (CCHP systems) and the impact of variations in their hardware components on overall costs and performance indicators.

Acknowledgements

This work is supported by Australian Government Research Training Program Scholarship (RTP) from Edith Cowan University. The support of Western Power, a Western Australian State Government owned corporation, is appreciated in assisting access to electric load data for the simulations undertaken. Cummins South Pacific and Optimal Group Australia Pty Ltd are also gratefully acknowledged for their technical advice in relation to combustion prime mover operational characteristics. Finally, Dr. Ganesh Kothapalli (Associate Supervisor, ECU) is also thanked for his comments during the PhD project.

Appendix A. Data used for system design and optimisation

Table A1
Stand-alone hybridised CHP system components cost, lifetime and emissions aspects.

Components	Description	Capital cost ($)	Replacement cost ($)	O & M cost ($/yr)	Life time (yr)	LCE (kg CO_2-eq/kW h)
PV module [4]	HS-PL135 (135 W)	310	310	0	25	0.05 [92]
ICE [97]	30 kW	10,500	10,500	260	10	0.88 [92]
MGT [98]	30 kW	75,300	75,300	1880	10	1.16 [99]
Battery [78]	12 V, 200 A h	419	419	11	10	0.03 [92]
Inverter [4]	1 kW	800	750	20	15	0 [92]
Charge controller [100]	1 kW	450	450	11	15	
Electric heater [101]	14.4 kW	1160	1160	28	5	
Heat exchanger [102]	Shell and tube, 8 m^2	9800	9800	245	10	
Discount rate		10%				
Fuel cost	Diesel fuel	0.91$/l				
	Natural gas	3.30$/GJ				

Appendix B. Power management strategy

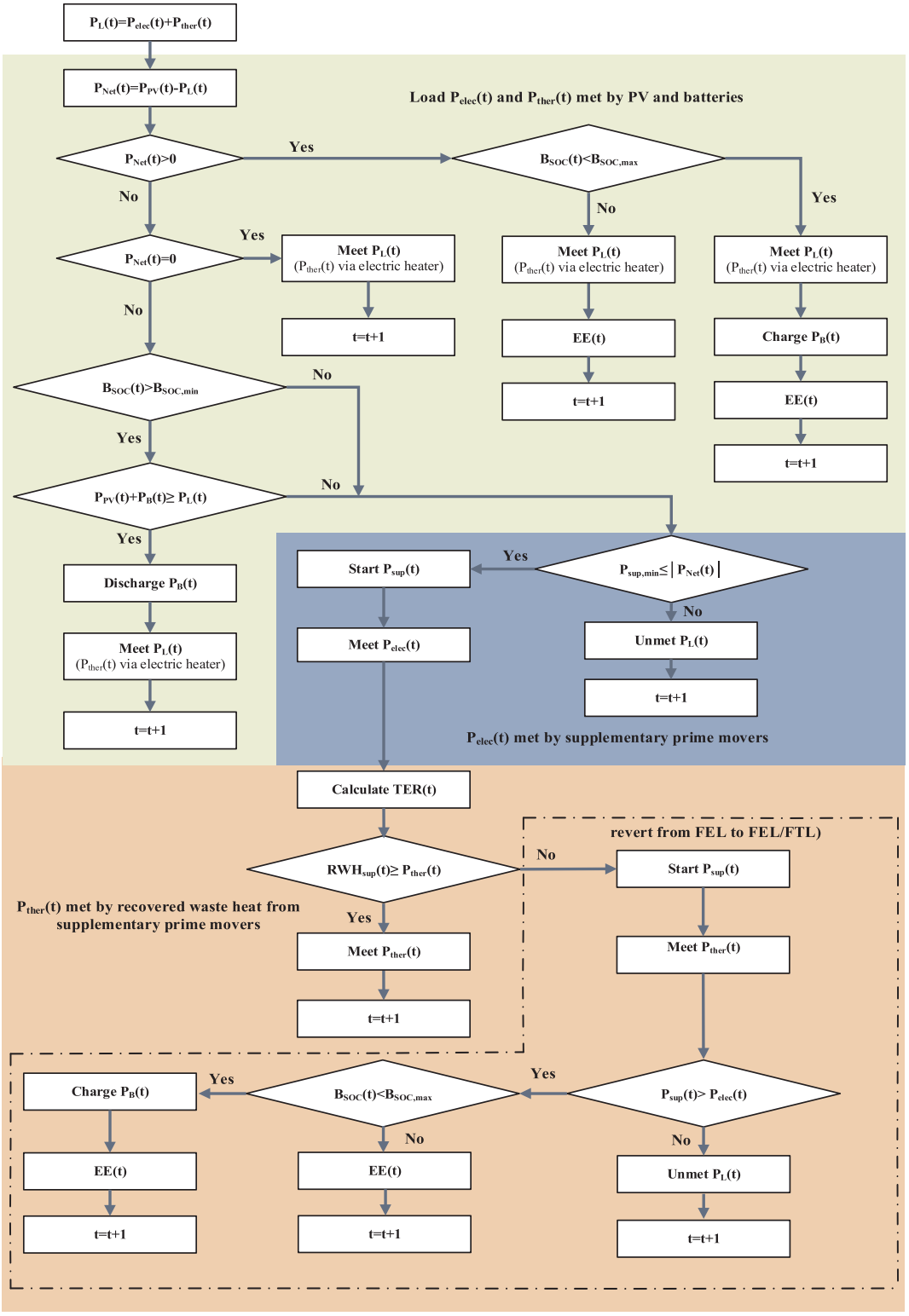

Fig. B1. Power Management Strategy (PMS) for meeting electricity (P_{elec} (t)) and heating demand (P_{ther} (t)).

Appendix C. Sensitivity analysis of GA population size

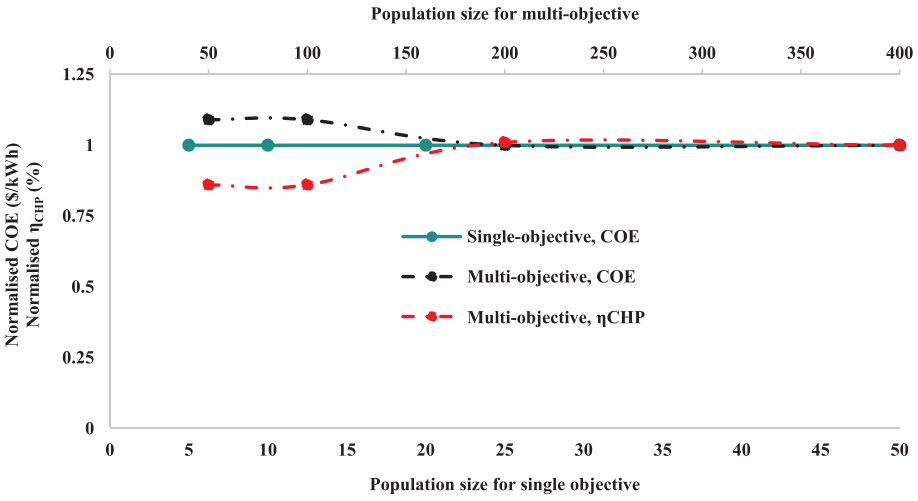

Fig. C1. Effect of population size on system optimisation for PV/Batt/ICE on FEL/FTL operating strategy at ETLR = 60:40.

Appendix D. PV modelling

The PV module's current based on the single diode equivalent circuit is defined by the following equation [76,77], whereby $I_L(t)$ is the light current, I_o is the diode reverse saturation current, $R_s(t)$ is the series resistance, R_{sh} is the shunt resistance, and $a(t)$ is the modified ideality factor.

$$I_{PV}(t) = I_L(t) - I_o\left[\exp\left(\frac{V + I_{PV}(t)R_s(t)}{a(t)}\right) - 1\right] - \frac{V + I_{PV}(t)R_s(t)}{R_{sh}} \quad \text{(D1)}$$

The light current $I_L(t)$ of PV module can be calculated using the Eq. (D2), where $S(t)$ is the solar irradiance, $T_{PV}(t)$ is the cell temperature, S_{ref} is the reference solar irradiation (1000 W/m^2), $I_{L,ref}$ is the short circuit current at the reference temperature (8.33 A), κ_t is the temperature coefficient of short circuit current (0.0005/°C), and T_{ref} is the reference temperature (25 °C) [71,72].

$$I_L(t) = \left(\frac{S(t)}{S_{ref}}\right)(I_{L,ref} + \kappa_t(T_{PV}(t) - T_{ref})) \quad \text{(D2)}$$

Additionally shunt resistance R_{sh} is calculated by the Eq. (D3), where V_{mp} is the maximum power point voltage, I_{mp} is the maximum power point current, V_{oc} is the nominal open circuit voltage, and I_{sc} is the short circuit current.

$$R_{sh} = \frac{V_{mp}}{I_{sc} - I_{mp}} - \frac{V_{oc} - V_{mp}}{I_{mp}} \quad \text{(D3)}$$

On the other hand, the cell temperature is determined by Eq. (D4) [103], where $T_{amb}(t)$ is the ambient temperature (°C), and $W_s(t)$ is the wind speed (m/s):

$$T_{PV}(t) = 0.943 \times T_{amb}(t) + 0.028 \times S(t) - 1.528 \times W_s(t) + 4.3 \quad \text{(D4)}$$

Appendix E. Battery modelling

The state of charge of lead acid battery at any time step (t) is the summation of state of charge at the previous time interval (t − 1) and the additional charge over the current time step (t) and is calculated by the Eq. (E1), whereas the battery state of charge during discharging can be calculated by Eq. (E2) [59,72], where C_b is the nominal capacity of the battery, $P_{PV}(t)$ is the power generation from PV module, $P_{sup}(t)$ is the power generation by supplementary prime movers, η_{inv} is the inverter efficiency, and Δt is the simulation time step (15 min).

$$B_{SOC}(t) = B_{SOC}(t-1) + \frac{\left((P_{PV}(t) + P_{sup}(t)) - \frac{P_L(t)}{\eta_{inv}}\right) \times \eta_b \times \Delta t}{C_b} \quad \text{(E1)}$$

$$B_{SOC}(t) = B_{SOC}(t-1) - \frac{\left(\frac{P_L(t)}{\eta_{inv}} - (P_{PV}(t) + P_{sup}(t))\right) \times \eta_b \times \Delta t}{C_b} \quad \text{(E2)}$$

In this study, the battery charging efficiency (η_b) is taken to be equal to the round trip efficiency of the battery and discharging efficiency (η_b) is set to 1 [57], and the battery state of charge is subjected to the following constraints at any time step (Δt):

$$B_{SOC,\min} \leqslant B_{SOC}(t) \leqslant B_{SOC,\max} \quad \text{(E3)}$$

References

[1] Kabalci E. Design and analysis of a hybrid renewable energy plant with solar and wind power. Energy Convers Manage 2013;72:51–9.
[2] Baghdadi F, et al. Feasibility study and energy conversion analysis of stand-alone hybrid renewable energy system. Energy Convers Manage 2015;105:471–9.
[3] Hoque SN, Das BK. Analysis of cost, energy and emission of solar home systems in Bangladesh. Int J Renewable Energy Res 2013;3(2):347–52.
[4] Brka A, Al-Abdeli YM, Kothapalli G. The interplay between renewables penetration, costing and emissions in the sizing of stand-alone hydrogen systems. Int J Hydrogen Energy 2015;40(1):125–35.
[5] Clarke DP, Al-Abdeli YM, Kothapalli G. The impact of renewable energy intermittency on the operational characteristics of a stand-alone hydrogen generation system with on-site water production. Int J Hydrogen Energy 2013;38(28):12253–65.
[6] Courtecuisse V, et al. A methodology to design a fuzzy logic based supervision of hybrid renewable energy systems. Math Comput Simul 2010;81(2):208–24.
[7] Brka A, Al-Abdeli YM, Kothapalli G. Predictive power management strategies for stand-alone hydrogen systems: Operational impact. Int J Hydrogen Energy 2016;41(16):6685–98.
[8] Zubi G, et al. Concept development and techno-economic assessment for a solar home system using lithium-ion battery for developing regions to provide electricity for lighting and electronic devices. Energy Convers Manage 2016;122:439–48.
[9] Najmul Hoque S, Kumar Das B. Present status of solar home and photovoltaic micro utility systems in Bangladesh and recommendation for further expansion and upgrading for rural electrification. J Renewable Sustainable Energy 2013;5(4):042301.
[10] Devrim Y, Bilir L. Performance investigation of a wind turbine–solar photovoltaic panels–fuel cell hybrid system installed at İncek region – Ankara, Turkey. Energy Convers Manage 2016;126:759–66.
[11] Bortolini M, Gamberi M, Graziani A. Technical and economic design of photovoltaic and battery energy storage system. Energy Convers Manage 2014;86:81–92.
[12] Das BK, et al. A techno-economic feasibility of a stand-alone hybrid power generation for remote area application in Bangladesh. Energy 2017;134:775–88.
[13] Clarke DP, Al-Abdeli YM, Kothapalli G. The impact of using particle swarm optimisation on the operational characteristics of a stand-alone hydrogen system with on-site water production. Int J Hydrogen Energy 2014;39(28):15307–19.
[14] Homayouni F, Roshandel R, Hamidi AA. Techno-economic and environmental analysis of an integrated standalone hybrid solar hydrogen system to supply CCHP loads of a greenhouse in Iran. Int J Green Energy 2017;14(3):295–309.
[15] Fux SF, Benz MJ, Guzzella L. Economic and environmental aspects of the component sizing for a stand-alone building energy system: A case study. Renewable Energy 2013;55:438–47.
[16] Lacko R, et al. Stand-alone renewable combined heat and power system with hydrogen technologies for household application. Energy 2014;77:164–70.
[17] Angrisani G, et al. Performance assessment of cogeneration and trigeneration systems for small scale applications. Energy Convers Manage 2016;125:194–208.
[18] Akikur R, et al. Performance analysis of a co-generation system using solar energy and SOFC technology. Energy Convers Manage 2014;79:415–30.
[19] Çakir U, Çomakli K, Yüksel F. The role of cogeneration systems in sustainability of energy. Energy Convers Manage 2012;63:196–202.
[20] Dorer V, Weber A. Energy and CO_2 emissions performance assessment of residential micro-cogeneration systems with dynamic whole-building simulation programs. Energy Convers Manage 2009;50(3):648–57.
[21] Liu M, Shi Y, Fang F. Combined cooling, heating and power systems: A survey. Renew Sustain Energy Rev 2014;35:1–22.
[22] Yao E, et al. Multi-objective optimization and exergoeconomic analysis of a combined cooling, heating and power based compressed air energy storage system. Energy Convers Manage 2017;138:199–209.
[23] Franco A, Versace M. Multi-objective optimization for the maximization of the operating share of cogeneration system in district heating network. Energy Convers Manage 2017;139:33–44.
[24] Zhang X, et al. Analysis of a feasible trigeneration system taking solar energy and biomass as co-feeds. Energy Convers Manage 2016;122:74–84.
[25] Yao E, et al. Thermo-economic optimization of a combined cooling, heating and power system based on small-scale compressed air energy storage. Energy Convers Manage 2016;118:377–86.
[26] Mojica JL, et al. Optimal combined long-term facility design and short-term operational strategy for CHP capacity investments. Energy 2017;118:97–115.
[27] Kaviri AG, et al. Exergoenvironmental optimization of heat recovery steam generators in combined cycle power plant through energy and exergy analysis. Energy Convers Manage 2013;67:27–33.
[28] Khaljani M, Saray RK, Bahlouli K. Comprehensive analysis of energy, exergy and exergo-economic of cogeneration of heat and power in a combined gas turbine and organic Rankine cycle. Energy Convers Manage 2015;97:154–65.
[29] Abusoglu A, Kanoglu M. Exergetic and thermoeconomic analyses of diesel engine powered cogeneration: Part 1–Formulations. Appl Therm Eng 2009;29(2):234–41.
[30] Rosen MA, Le MN, Dincer I. Efficiency analysis of a cogeneration and district energy system. Appl Therm Eng 2005;25(1):147–59.
[31] Balli O, Aras H, Hepbasli A. Thermodynamic and thermoeconomic analyses of a trigeneration (TRIGEN) system with a gas–diesel engine: Part II–An application. Energy Convers Manage 2010;51(11):2260–71.
[32] ASHRAE, P., 2008. Heating and cooling, ASHRAE handbook-HVAC systems and equipment, SI ed. American Society of Heating Refrigerating and Air-Conditioning Engineers (ASHRAE) Atlanta, GA, US.
[33] Khatri KK, et al. Experimental investigation of CI engine operated micro-trigeneration system. Appl Therm Eng 2010;30(11):1505–9.
[34] Ahmadi P, Rosen MA, Dincer I. Greenhouse gas emission and exergo-environmental analyses of a trigeneration energy system. Int J Greenhouse Gas Control 2011;5(6):1540–9.
[35] Ghaebi H, Saidi M, Ahmadi P. Exergoeconomic optimization of a trigeneration system for heating, cooling and power production purpose based on TRR method and using evolutionary algorithm. Appl Therm Eng 2012;36:113–25.
[36] Caresana F, et al. Use of a test-bed to study the performance of micro gas turbines for cogeneration applications. Appl Therm Eng 2011;31(16):3552–8.
[37] Onovwiona HI, Ugursal VI, Fung AS. Modeling of internal combustion engine based cogeneration systems for residential applications. Appl Therm Eng 2007;27(5):848–61.
[38] Kusakana K, Vermaak HJ. Hybrid diesel generator/renewable energy system performance modeling. Renewable Energy 2014;67:97–102.
[39] Ismail M, Moghavvemi M, Mahlia T. Genetic algorithm based optimization on modeling and design of hybrid renewable energy systems. Energy Convers Manage 2014;85:120–30.
[40] Abdollahi G, Sayyaadi H. Application of the multi-objective optimization and risk analysis for the sizing of a residential small-scale CCHP system. Energy Build 2013;60:330–44.
[41] Wang J-J, Jing Y-Y, Zhang C-F. Optimization of capacity and operation for CCHP system by genetic algorithm. Appl Energy 2010;87(4):1325–35.
[42] Ahmadi P, et al. Multi-objective optimization of a combined heat and power (CHP) system for heating purpose in a paper mill using evolutionary algorithm. Int J Energy Res 2012;36(1):46–63.
[43] Borji M, et al. Parametric analysis and Pareto optimization of an integrated autothermal biomass gasification, solid oxide fuel cell and micro gas turbine CHP system. Int J Hydrogen Energy 2015;40(41):14202–23.
[44] Pirkandi J, et al. Simulation and multi-objective optimization of a combined heat and power (CHP) system integrated with low-energy buildings. J Build Eng 2016;5:13–23.
[45] Mohammadi-Ivatloo B, Moradi-Dalvand M, Rabiee A. Combined heat and power economic dispatch problem solution using particle swarm optimization with time varying acceleration coefficients. Electric Power Syst Res 2013;95:9–18.
[46] Moradi MH, et al. An energy management system (EMS) strategy for combined heat and power (CHP) systems based on a hybrid optimization method employing fuzzy programming. Energy 2013;49:86–101.
[47] Wang J, et al. Particle swarm optimization for redundant building cooling heating and power system. Appl Energy 2010;87(12):3668–79.
[48] Clarke DP, Al-Abdeli YM, Kothapalli G. Multi-objective optimisation of renewable hybrid energy systems with desalination. Energy 2015;88:457–68.
[49] Seijo S, et al. Modeling and multi-objective optimization of a complex CHP process. Appl Energy 2016;161:309–19.
[50] Ebrahimi M, Keshavarz A. Sizing the prime mover of a residential micro-combined cooling heating and power (CCHP) system by multi-criteria sizing method for different climates. Energy 2013;54:291–301.
[51] Hajabdollahi H, Ganjehkaviri A, Jaafar MNM. Assessment of new operational strategy in optimization of CCHP plant for different climates using evolutionary algorithms. Appl Therm Eng 2015;75:468–80.
[52] Mago PJ, Hueffed AK. Evaluation of a turbine driven CCHP system for large office buildings under different operating strategies. Energy Build 2010;42(10):1628–36.
[53] Mostofi M, Nosrat A, Pearce JM. Institutional scale operational symbiosis of photovoltaic and cogeneration energy systems. Int J Environ Sci Technol 2011;8(1):31–44.
[54] Brandoni C, Renzi M. Optimal sizing of hybrid solar micro-CHP systems for the household sector. Appl Therm Eng 2015;75:896–907.
[55] Basrawi F, Yamada T, Obara Sy. Economic and environmental based operation strategies of a hybrid photovoltaic–microgas turbine trigeneration system. Appl Energy 2014;121:174–83.
[56] Borowy BS, Salameh ZM. Methodology for optimally sizing the combination of a

battery bank and PV array in a wind/PV hybrid system. Energy Convers, IEEE Trans 1996;11(2):367–75.
[57] Yang H, et al. Optimal sizing method for stand-alone hybrid solar–wind system with LPSP technology by using genetic algorithm. Sol Energy 2008;82(4):354–67.
[58] Belmili H, et al. Sizing stand-alone photovoltaic–wind hybrid system: Techno-economic analysis and optimization. Renew Sustain Energy Rev 2014;30:821–32.
[59] Nafeh AE-SA. Optimal economical sizing of a PV-wind hybrid energy system using genetic algorithm. Int J Green Energy 2011;8(1):25–43.
[60] Cho H, et al. Evaluation of CCHP systems performance based on operational cost, primary energy consumption, and carbon dioxide emission by utilizing an optimal operation scheme. Appl Energy 2009;86(12):2540–9.
[61] Pfeifer A, et al. Economic feasibility of CHP facilities fueled by biomass from unused agriculture land: Case of Croatia. Energy Convers Manage 2016;125:222–9.
[62] Daghigh R, Shafieian A. An investigation of heat recovery of submarine diesel engines for combined cooling, heating and power systems. Energy Convers Manage 2016;108:50–9.
[63] Karellas S, Braimakis K. Energy–exergy analysis and economic investigation of a cogeneration and trigeneration ORC–VCC hybrid system utilizing biomass fuel and solar power. Energy Convers Manage 2016;107:103–13.
[64] Calise F, et al. Exergetic and exergoeconomic analysis of a novel hybrid solar–geothermal polygeneration system producing energy and water. Energy Convers Manage 2016;115:200–20.
[65] Das BK, Al-Abdeli YM, Kothapalli G. Optimisation of stand-alone hybrid energy systems supplemented by combustion-based prime movers. Appl Energy 2017;196:18–33.
[66] Costa A, Fichera A. A mixed-integer linear programming (MILP) model for the evaluation of CHP system in the context of hospital structures. Appl Therm Eng 2014;71(2):921–9.
[67] Ghadimi PS, Kara S, Kornfeld B. The optimal selection of on-site CHP systems through integrated sizing and operational strategy. Appl Energy 2014;126(Supplement C):38–46.
[68] Ipsakis D, et al. Power management strategies for a stand-alone power system using renewable energy sources and hydrogen storage. Int J Hydrogen Energy 2009;34(16):7081–95.
[69] Long WC, Luck R, Mago PJ. Uncertainty based operating strategy selection in combined heat and power systems. Appl Therm Eng 2016;98:1013–24.
[70] Smith AD, Mago PJ. Effects of load-following operational methods on combined heat and power system efficiency. Appl Energy 2014;115(Supplement C):337–51.
[71] Solarshopnet. Technical data heckert HS-PL 135. Available from: 05.11.2016. http://www.solarshop-erope.net/solar-components/solarmodules/heckert_hs_pl-135_m_634.html.
[72] Clarke DP, Al-Abdeli YM, Kothapalli G. The effects of including intricacies in the modelling of a small-scale solar-PV reverse osmosis desalination system. Desalination 2013;311:127–36.
[73] BOM. Western Australia weather and warnings. Available from: 12.10.2015. http://reg.bom.gov.au/climate/reg/oneminsolar/.
[74] Kashefi Kaviani A, Riahy GH, Kouhsari SM. Optimal design of a reliable hydrogen-based stand-alone wind/PV generating system, considering component outages. Renewable Energy 2009;34(11):2380–90.
[75] Shabani B, Andrews J, Watkins S. Energy and cost analysis of a solar-hydrogen combined heat and power system for remote power supply using a computer simulation. Sol Energy 2010;84(1):144–55.
[76] Deshmukh SS, Boehm RF. Review of modeling details related to renewably powered hydrogen systems. Renew Sustain Energy Rev 2008;12(9):2301–30.
[77] Duffie JA, Beckman WA. Solar engineering of thermal processes vol. 3. New York: Wiley; 1980.
[78] Lead-acid battery. Available from: 20.11.2015. http://www.sunstonepower.com/upload/userfiles/files/ML12-200.pdf.
[79] Kim H-S, et al. High-efficiency isolated bidirectional AC–DC converter for a DC distribution system. IEEE Trans Power Electron 2013;28(4):1642–54.
[80] Cummins South Pacific (12.10.2015). B3.3 Engine Data Sheet & Performance Curve (30kW FR 30002). Source: Personal Communication.
[81] Technical Reference: Capstone Model C30 Performance. Available from: 15.11. 2015. http://www.wmrc.edu/projects/bar-energy/manuals/c-30-manuals/410004_Model_C30_Performance.pdf.
[82] Infield D, et al. Review of wind/diesel strategies. IEE Proc A (Phys Sci, Meas Instrum, Manage Educ, Rev), 1983; 130(9): 613–9.
[83] Hoevenaars EJ, Crawford CA. Implications of temporal resolution for modeling renewables-based power systems. Renewable Energy 2012;41:285–93.
[84] Darrow K. et al., Catalog of CHP technologies; 2014.
[85] Wiehagen J, Sikora J. Performance comparison of residential hot water systems. Upper Marlboro, Maryland, NREL: NAHB Research Center; 2003.
[86] Aguilar C, White D, Ryan DL. Domestic water heating and water heater energy consumption in Canada. Canadian Building Energy End-Use Data and Analysis Centre; 2005.
[87] Arun P, Banerjee R, Bandyopadhyay S. Optimum sizing of battery-integrated diesel generator for remote electrification through design-space approach. Energy 2008;33(7):1155–68.
[88] Dufo-López R, et al. Multi-objective optimization minimizing cost and life cycle emissions of stand-alone PV–wind–diesel systems with batteries storage. Appl Energy 2011;88(11):4033–41.
[89] Srinivas N, Deb K. Muiltiobjective optimization using nondominated sorting in genetic algorithms. Evolutionary Comput 1994;2(3):221–48.
[90] Wang J, et al., Multi-objective optimization of an organic Rankine cycle (ORC) for low grade waste heat recovery using evolutionary algorithm. Energy Convers Manage 2013; 71(Supplement C): 146–58.
[91] Tezer T, Yaman R, Yaman G. Evaluation of approaches used for optimization of stand-alone hybrid renewable energy systems. Renew Sustain Energy Rev 2017;73:840–53.
[92] Katsigiannis Y, Georgilakis P, Karapidakis E. Multiobjective genetic algorithm solution to the optimum economic and environmental performance problem of small autonomous hybrid power systems with renewables. Renewable Power Generation, IET 2010;4(5):404–19.
[93] Soltani R, et al. Multi-objective optimization of a solar-hybrid cogeneration cycle: application to CGAM problem. Energy Convers Manage 2014;81:60–71.
[94] Wang J, et al. Multi-objective optimization of an organic Rankine cycle (ORC) for low grade waste heat recovery using evolutionary algorithm. Energy Convers Manage 2013;71:146–58.
[95] Ahmadi P, Dincer I, Rosen MA. Thermodynamic modeling and multi-objective evolutionary-based optimization of a new multigeneration energy system. Energy Convers Manage 2013;76:282–300.
[96] Pierobon L, et al. Multi-objective optimization of organic Rankine cycles for waste heat recovery: Application in an offshore platform. Energy 2013;58:538–49.
[97] Central Maine Diesel. Available from: 03.02.2016. http://www.centralmainediesel.com/cummins-generators.asp.
[98] Combine heat and power partnership. Catalog of CHP technologies. U.S. Environmental Protection Agency; 2015. p. 1–6, 5.1–5.18.
[99] Brown Jr EG. Life cycle assessment of existing and emerging distributed generation technologies in California; 2011.
[100] Ismail MS, Moghavvemi M, Mahlia TMI. Design of an optimized photovoltaic and microturbine hybrid power system for a remote small community: Case study of Palestine. Energy Convers Manage 2013;75:271–81.
[101] Electric Water Heater. Available from: 10.06.2017 https://1stchoicehotwater.com.au/product/rheem-heavy-duty-electric-613050g7-50l/.
[102] Lin C-S. Capture of heat energy from diesel engine exhaust; 2008. Available from: 10.02.2017 https://www.osti.gov/scitech/servlets/purl/963351.
[103] Tamizh Mani G, et al. Photovoltaic module thermal/wind performance: long-term monitoring and model development for energy rating. In: Proc. NCPV and solar program review meeting; 2003. p. 936–9.